COOMET Supplementary Comparison on

Wavelength for Fiber Optics

COOMET PR-S8

(COOMET project # 689/RU/16)

Final Report

Vladimir Kravtsov, Alexey Mitiurev
All-Russian Research Institute for Optical and Physical Measurements (VNIIOFI),
Ozernaya 46, 119361, Moscow, Russia

Correspondence to: kravtsov-f3@vniiofi.ru, mak@vniiofi.ru

2019

Moscow

COOMET Supplementary Comparison on Wavelength for Fiber Optics

Abstract

BelGIM, NIM, NIS, NMISA, PTB and VNIIOFI carried out the supplementary comparison on the wavelength for fiber optics. The aim of this comparison is to examine the equivalence of the wavelength for fiber optics among participating laboratories and to provide supporting evidence for the associated CMC claims in BIPM KCDB.

Table of Contents

1 Introduction

This report presents the results of the comparison project COOMET.PR-S8 – international supplementary comparison of wavelength for fiber, piloted by VNIIOFI. The comparison is performed according to the Guideline for CCPR Key Comparison Report Preparation which is issued by the CCPR Working Group on Key Comparisons CCPR-G2 [1].

The technical protocol was prepared by VNIIOFI and agreed by the other participants. The comparison was carried out through the calibration of the VNIIOFI artifact which is based on a Hydrogen Cyanide ($H^{13}C^{14}N$) gas cell with absorption peaks within the wavelength range from 1525 to 1565 nm. More details are in the Technical Protocol of the COOMET.PR-S8 comparison.

2 Organization

2.1 Participants

2.1.1 VNIIOFI acted as a pilot laboratory among the participants in this international comparison.

2.1.2 BelGIM in cooperation with Institute of Physics of the NAS of Belarus (Belarus); NIM (China); PTB (Germany); INMETRO (Brazil); NMISA (South Africa); and VNIIOFI (Russia) (full names and addresses are in the table 2.2.1) were the initial participants of the comparison according to the Technical Protocol. All the participants confirmed the intention to take part in the COOMET Project.

2.1.3 The comparison measurements started in May 2016 with six participants.

NIS (Egypt) joined the Project at the finishing stage of measurements, all the participants agreed with this. NIS is included in the table 2.1 as additional organization as compared to the initial technical protocol.

The predraft A materials based on participants reports were prepared by the pilot. They were submitted and discussed by all the participants. Some uncertainty values were changed (not less than initial) by VNIIOFI and PTB after additional analysis and accepted by all participants at this stage. All the participants approved the possibility of adding s^2 uncertainty according to paragraph 4 of the Guidelines [1], and of excluding data of a participant with great deviation from the tentative CRV calculations.

At the finish of predraft A materials discussion INMETRO decided to discontinue participation in the project because of mistakes in measurement results which were found during the additional analysis in Brazil.

So this report presents the results of six participants: BelGIM in cooperation with Institute of Physics of the NAS of Belarus (Belarus); NIM (China); NIS (Egypt); NMISA (South Africa); PTB (Germany) and VNIIOFI (Russia).

2.1.4 All the participants were able to demonstrate traceability to an independent realization of the quantity, or to make clear the route of traceability to the quantity via another named laboratories at the time of comparison measurements.

2.2 Participant Details

Table 2-1 – Contact list of participants

<table>
<tr><th>№</th><th>Parti-
cipants</th><th>Correspon-
dence</th><th>E-mail address
Phone number</th><th>Address</th><th>Remarks</th></tr>
<tr><td rowspan="2">1</td><td rowspan="2">BelGIM
(Belarus)</td><td>Yury Shershun</td><td>yshershun@belgim.by
+375 17 335 5069</td><td>Republican Unitary Enterprise “Belarusian State Institute of Metrology” – BelGIM, 93, Starovilensky trakt, Minsk, 220053, Belarus</td><td></td></tr>
<tr><td>Anatoliy Isaevich</td><td>a.isaevich@ifanbel.bas-net.by
+375 17 284 0507</td><td>The State Scientific Institution «B.I.Stepanov Institute of Physics of the National Academy of Sciences of Belarus» – Institute of Physics of the NAS of Belarus, 68-2, Nezalezhnasti Ave., Minsk, 220072, Belarus</td><td></td></tr>
<tr><td>2</td><td>NIM
(China)</td><td>Xu Nan

Lin Yandong</td><td>xunan@nim.ac.cn
+86-10-64524823
linyd@nim.ac.cn;
+86-10-64524805</td><td>Division of Optics, National Institute of Metrology (NIM)
18 Bei San Huan Dong Lu, Chaoyang Dist., Beijing 100029, P.R.China</td><td></td></tr>
<tr><td>3</td><td>PTB
(Germany)</td><td>Stefan Kueck</td><td>Stefan.Kueck@ptb.de
+49 531 592 4100</td><td>Physikalisch-Technische Bundesanstalt (PTB) Department Photometry and Applied Radiometry
Bundesallee 100 38116 Braunschweig Germany</td><td></td></tr>
<tr><td>4</td><td>INMETRO
(Brazil)</td><td>Giovanna Borghi</td><td>gbalmeida@inmetro.gov.br
+55 (21) 2679-9051</td><td>National Institute of Metrology, Quality and Technology (INMETRO)
Santa Alexandrina St, 416 Rio Comprido - Rio de Janeiro - RJ - Brazil
Zip Code: 20261-232</td><td>Withdrew and excluded</td></tr>
<tr><td>5</td><td>NMISA
(South Africa)</td><td>Mariesa Nel</td><td>MNel@nmisa.org
+ 27 12 841 2561</td><td>National Metrology Institute of South Africa (NMISA)
Private Bag X34, Lynnwood Ridge, Pretoria, 0040, South Africa</td><td></td></tr>
<tr><td>6</td><td>NIS
(Egypt)</td><td>Osama Terra</td><td>osama.terra@gmail.com
osama.terra@nis.sci.eg
+20 1141172900</td><td>Primary length standard and laser technology lab.
National Institute of standards
Tersa street, Haram, Giza, Egypt
P.O.Box 136 Giza, code 12211</td><td>Added</td></tr>
<tr><td>7</td><td>VNIIOFI
(Russia)
Pilot</td><td>Vladimir Kravtsov

Aleksey Mitiurev</td><td>kravtsov-f3@vniiofi.ru
+7 495 781-45-86

mak@vniiofi.ru
+7 495 781-45-83</td><td>Low Intensity Lasers Radiation and Fiber Optical Systems Metrology Laboratory, All Russian Research Institute for Optical and Physical Measurements (VNIIOFI)
Ozernaya st.46, Moscow, 119361, Russia</td><td></td></tr>
</table>

2.3 Form of Comparison

2.3.1 The comparison was carried out through calibrations of the artifact based on a Hydrogen Cyanide ($H^{13}C^{14}N$) gas cell with absorption peaks within wavelength range from 1525 to 1565 nm. Artifact was prepared by VNIIOFI. The artifact contains one gas cell. The artifact has an input and output FC/APC type connectors.

2.3.2 Sequence of measurements was:

Pilot – Participant 1 – Participant 2 – …. – Pilot.

2.3.3 The comparison had one round. Each participant had two months period for measurements and one month period for delivering of the artifact to the next participant. There were no problems with the artifact during the transportation.

2.4 Timetable

Comparison timetable from the technical protocol is ~~as~~ shown in the following table.

Table 2-2 – Scheduled timetable of the comparison at the beginning

Activity	Start Date	End Date
First measurement at VNIIOFI	01 May, 2016	15 June, 2016
Delivery to BelGIM	15 June, 2016	15 July, 2016
Measurement at BelGIM	15 July, 2016	15 September , 2016
Delivery to NIM	15 September , 2016	15 October, 2016
Measurement at NIM	15 October, 2016	15 December, 2016
Delivery to INMETRO	15 December, 2016	31 January, 2017
Measurement at INMETRO	1 February , 2017	31 March, 2017
Delivery to NMISA	01 April, 2017	30 April, 2017
Measurement at NMISA	01 May, 2017	30 June, 2017
Delivery to PTB	01 July, 2017	31 July, 2017
Measurement at PTB	01 August, 2017	30 September, 2017
Delivery to VNIIOFI	01 October, 2017	31 October, 2017
Second measurement at VNIIOFI	01 November, 2017	31 December, 2017
Distribution of Pre-Draft A data	15 January, 2018	31 March, 2018
Distribution Draft A	31 May, 2018	

There was a modification to the scheduled timetable because of NIS, Egypt participation to the comparison. NIS made their measurements after PTB. So there was a delay in the schedule of comparisons due to the time needed by NIS for transportation, customs clearance, measurement and report preparation. Participants submitted measurements results (reports) to the pilot mostly within two months after completion of theirs measurements.

VNIIOFI made finishing measurements and prepared its data by April 2018. All the comparison reports from participants were gathered by VNIIOFI by the end of May 2018.

3 Description of the Artifact

3.1 The artifact is based on a Hydrogen Cyanide ($H^{13}C^{14}N$) gas cell produced by Wavelength References Company for spectral range 1525 – 1565 nm (C-range) with FC/APC connectors. This cell is packed into the plastic case with FC adapters.

3.2 General view of the cell and package is shown in the figures below.

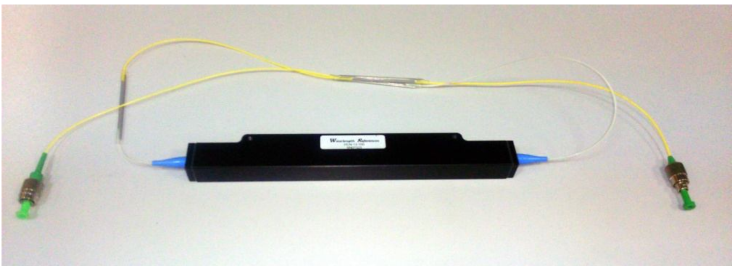

Fig. 3-1 – General view of the artifact

Fig. 3-2 – General view of the cell package

4 Measurement Capability and Results of Pilot Laboratory

4.1 Scheme and measurement procedure

4.1.1 Measurement setup is based on tunable laser with high accuracy wavelength meter and power meter (see fig. 4-1). The principle is to find out minimum average power of laser radiation going through the cell for several absorption peaks with corresponding wavelengths. Absorption peaks of hydrogen cyanide $H^{13}C^{14}N$ under investigation were: R26, R24, R16, R08, R0, P05, P10, P16, P24, and P26.

4.1.2 Before connecting the artifact to the participant's measurement setup, the FC/APC connector ends of both the artifact and the setup were inspected if there is any dust, contamination, or damage.

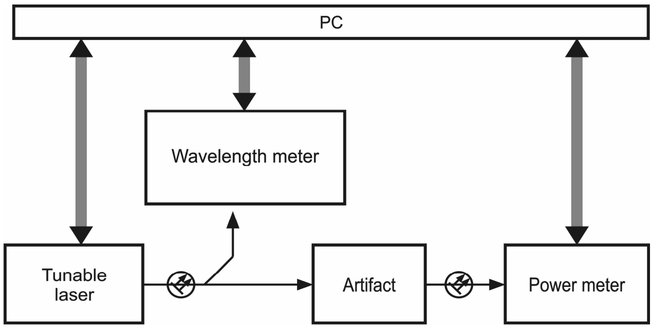

Fig. 4-1 – Schematic diagram of measurement setup for Wavelength comparison

Fig. 4-2 – Photo of measurement setup for Wavelength comparison

The laboratory environmental conditions were: temperature (23 ± 5) °C and humidity less than 70%. The artifact was located into temperature-controlled chamber during the measurements with temperature of (23 ± 0,5) °C.

4.2 Traceabililty

The Wavelength Meter (Angstrom IR WS-2) was used for the measurement of the laser wavelengths and was calibrated by reference cavity stabilized laser at λ_{ref} = 1542 nm. The optical power meter EXFO PM-1600 was used for relative power measurements. The power meter was calibrated by the working metrological standard RESM - VS.

4.3 Results

Table 4-1 – Components of uncertainty

Uncertainty source	Type	Symbols
The standard deviation of the result of measurements of the mean value of the wavelength	A	u_λ
Wavelength meter uncertainty	B	u_{st}
Line fitting uncertainty	B	u_f
Combined standard uncertainty		u_c
Expanded uncertainty (k = 2, P = 95 %)		U_c

Table 4-2 – First measurement results and uncertainties

Wavelength peak	λ, nm	u_λ, pm	u_{st} pm	u_f pm	u_c pm	U pm
R26	1527,6335	0,097	0,124	0,200	0,254	0,508
R24	1528,4858	0,029	0,124	0,200	0,237	0,474
R16	1532,2831	0,035	0,124	0,200	0,238	0,476
R08	1536,7037	0,029	0,124	0,200	0,237	0,474
R00	1541,7526	0,044	0,125	0,200	0,240	0,480
P05	1545,9557	0,051	0,125	0,200	0,241	0,482
P10	1549,7302	0,043	0,125	0,200	0,240	0,480
P16	1554,5903	0,017	0,126	0,200	0,237	0,474
P24	1561,6352	0,092	0,126	0,200	0,254	0,508
P26	1563,4989	0,107	0,126	0,200	0,260	0,520

Table 4-3 – Second measurement results and uncertainties

Wavelength peak	λ, nm	u_λ, pm	u_{st} pm	u_f pm	u_c pm	U pm
R26	1527,6336	0,260	0,124	0,200	0,352	0,704
R24	1528,4860	0,054	0,124	0,200	0,243	0,486
R16	1532,2829	0,089	0,124	0,200	0,253	0,506
R08	1536,7036	0,054	0,124	0,200	0,244	0,488
R00	1541,7529	0,107	0,125	0,200	0,261	0,522
P05	1545,9559	0,065	0,125	0,200	0,247	0,494
P10	1549,7303	0,091	0,125	0,200	0,255	0,510
P16	1554,5905	0,085	0,126	0,200	0,253	0,506
P24	1561,6358	0,173	0,126	0,200	0,295	0,590
P26	1563,4987	0,085	0,126	0,200	0,253	0,506

Expanded uncertainty is derived by multiplying the combined standard uncertainty by coverage factor k = 2, that corresponds to the confidence level P approximately equal 95 % with assuming normal distribution. Uncertainty assessment is carried out according to ISO/IEC Guide

98-3:2008 “Measurement uncertainty – Part 3: Guide on measurement uncertainty expression (GUM: 1995)” [2].

\

5 Reporting Results and Uncertainties of participants

5.1 Belgim

5.1.1 Scheme and measurement procedure

Schematic diagram of measurement apparatus is shown in Fig. 5-1. Light from a tunable diode laser is sent through two beam splitters and an absorption cell to the detector. A part of the radiation from the first beam splitter was fed to the wavelength meter. A part of the radiation from the second beam splitter was fed to a second detector, which controlled the laser power. A computer controlled the laser radiation wavelength scan and recorded the readings of the two detectors and wavelength meter.

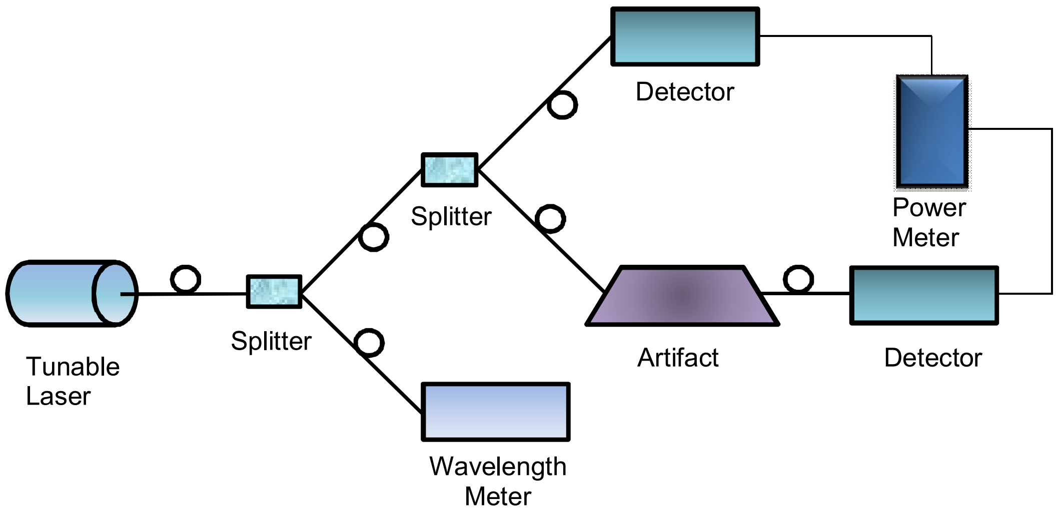

Fig. 5-1 – Measurement scheme for the comparisons

5.1.2 Traceability

The Wavelength Meter (Angstrom IR WS-U) was used for the measurement of the laser wavelengths and was calibrated by National standards of the Republic of Belarus NSRB 12-03. The reference optical tester OT-3-2 was used for relative power measurements. The reference optical tester was calibrated by National standards of the Republic of Belarus NSRB 25-15.

5.1.3 Results

Table 5-1 – Components of uncertainty and the expanded uncertainty

Uncertainty source	Type	Symbols
The standard deviation of the result of measurements of the mean value of the wavelength	A	u_λ
Wavelength meter uncertainty	B	u_{st}
Uncertainty due to interference fringes and other	B	u_r

Uncertainty source	Type	Symbols
sources of background variation		
Uncertainty of the approximation of the absorption line contour taking into account the uncertainty of measurement of the relative radiation power	B	u_f
Uncertainty due to changes in ambient temperature *	B	u_T
Combined standard uncertainty		u_c
Expanded uncertainty (k = 2, P = 95 %)		U_c
*$u_T \approx 0$ in accordance with W. C. Swann and S. L. Gilbert "Line centers, pressure shift, and pressure broadening of 1530–1560 nm hydrogen cyanide wavelength calibration lines," J. Opt. Soc. Am. B **22**,1749-1756 (2005) [3]		

Table 5-2 – Components of uncertainty and the expanded uncertainty

Wavelength peak	u_λ, pm	u_{st} pm	u_r pm	u_f pm	u_c pm	U_c pm
R26	0,051	0,092	0,020	0,029	0,111	0,222
R24	0,071	0,092	0,020	0,024	0,120	0,240
R16	0,043	0,092	0,020	0,022	0,106	0,212
R08	0,079	0,092	0,020	0,020	0,125	0,249
R00	0,072	0,093	0,020	0,028	0,122	0,244
P05	0,056	0,093	0,020	0,021	0,112	0,225
P10	0,052	0,093	0,020	0,019	0,110	0,220
P16	0,068	0,093	0,020	0,025	0,120	0,239
P24	0,037	0,094	0,020	0,027	0,106	0,213
P26	0,084	0,094	0,020	0,022	0,129	0,259

Expanded uncertainty is derived by multiplying the combined standard uncertainty by coverage factor k = 2, that corresponds to the confidence level P approximately equal 95 % with assuming normal distribution.

Uncertainty assessment is carried out according ISO/IEC Guide [2].

5.2 NIM

5.2.1 Scheme and measurement procedure

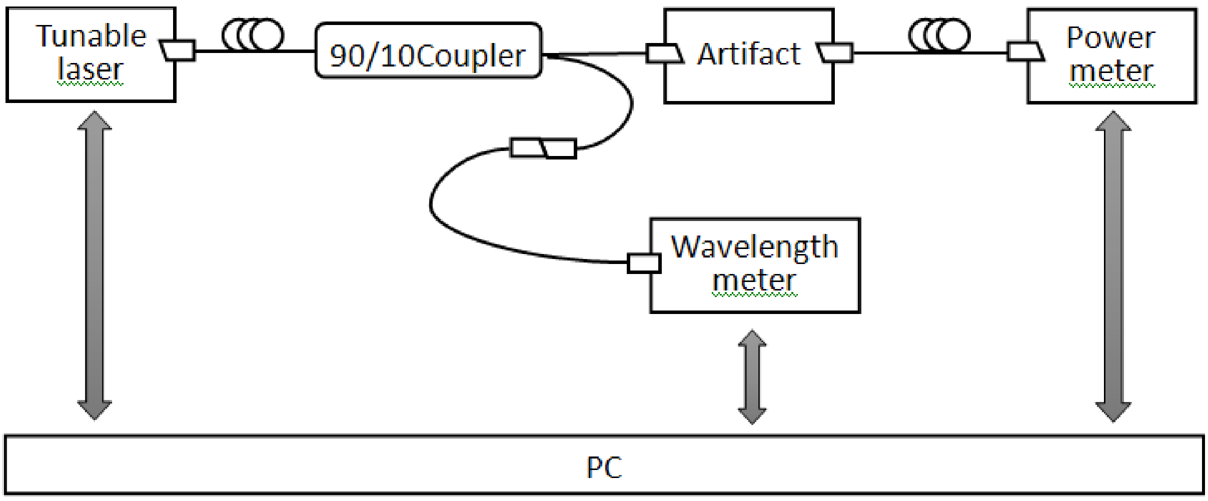

Fig. 5-2 – Schematic diagram of the measurement facility of NIM

Light from the tunable laser source was split into two paths with a splitting ratio of 90:10 by a broadband fiber optic coupler. 90% of light was delivered into the power meter through the artifact to measure the light power, and 10 % of light was delivered into the wavelength meter to measure the light wavelength. In Fig. 5-2, the vertical line in the small rectangle indicates FC/PC interface and the slanted line FC/APC interface.

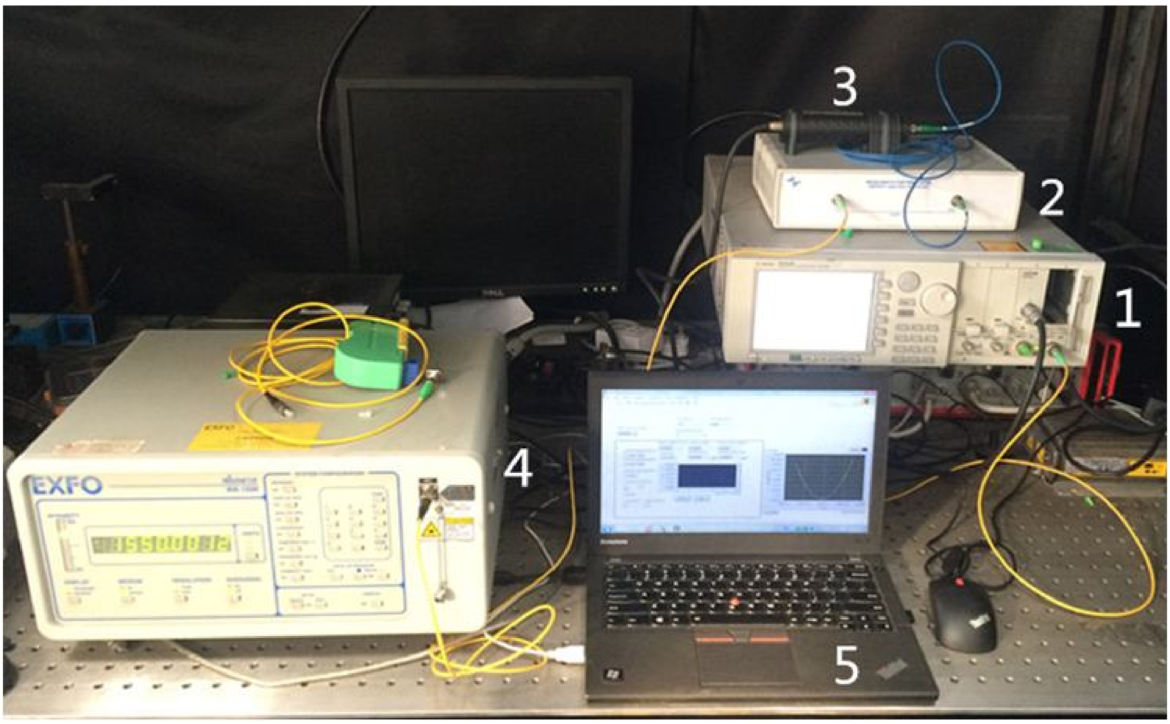

Fig. 5-3 – General view of measurement set-up for calibration of comparison artifact

(1) Agilent 81640A tunable laser source. (2) Comparison artifact. (3) Agilent 81623A optical power meter. (4) EXFO WA-1500 wavelength meter. (5) PC and software.

5.2.2 Traceability

The standard wavelength meter was calibrated at 633nm, 1314nm and 1542nm. For 633nm, it is calibrated using iodine-stabilized laser which is NIM's wavelength primary standard participated in BIPM.L-K11 comparison. For other wavelengths, the wavelength meter was calibrated using a CH_4-stabilized reference laser at 1314.58813nm, and a $^{13}C_2H_2$-stabilized reference laser at 1542.38371nm. The CH_4 and $^{13}C_2H_2$-stabilized reference lasers were built according to the linear absorption method.

5.2.3 Results

The following potential contributions were considered negligible or not relevant uncertainties:

Linearity of fiber power meter: Because the max absorption line depth of comparison artifact (R8 line and 16.5cm gas cell) is about 3,2 dB, linearity of fiber power meter within this range is negligible.

Temperature mismatch: All the measurements were done at a temperature of (23±0.5) C, and measurement results changes within measurement uncertainty at different temperatures. So contribution induced by the temperature is negligible.

The sources of uncertainty for the absorption peaks were reproducibility, nearby line contribution, background slop, line fitting statistics and standard wavelength meter uncertainty.

Table 5-3 – Components of uncertainty and the combined expanded uncertainty

Source	Type	Probability distribution	Relative standard uncertainty (nm)	Degree of freedom
Reproducibility	A	t	0,00006	8
Nearby line contribution	B	rectangular	0,00002	50
Background slope	B	rectangular	0,00006	50
Line fitting Statistics	B	rectangular	0,00005	50
Wavelength meter uncertainty	B	normal	0,00020	∞
Combined standard uncertainty		normal	0,00023	ν_{eff} = 1250
Expanded uncertainty (Level of Confidence 95%)			0,00044	k=1,96

5.3 NMISA

5.3.1 Scheme and measurement procedure

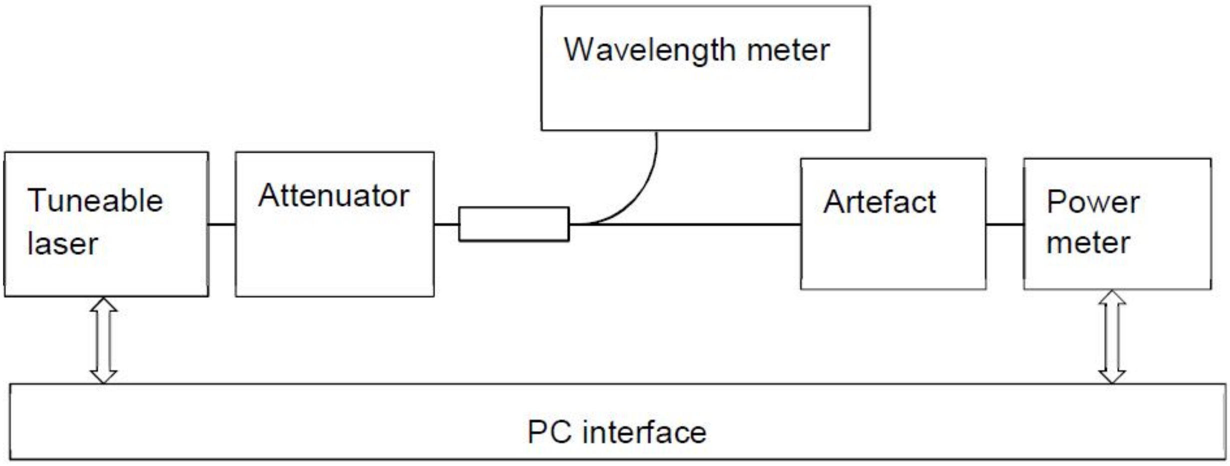

Fig. 5-4 – Schematic diagram of the measurement setup at NMISA fibre optic laboratory

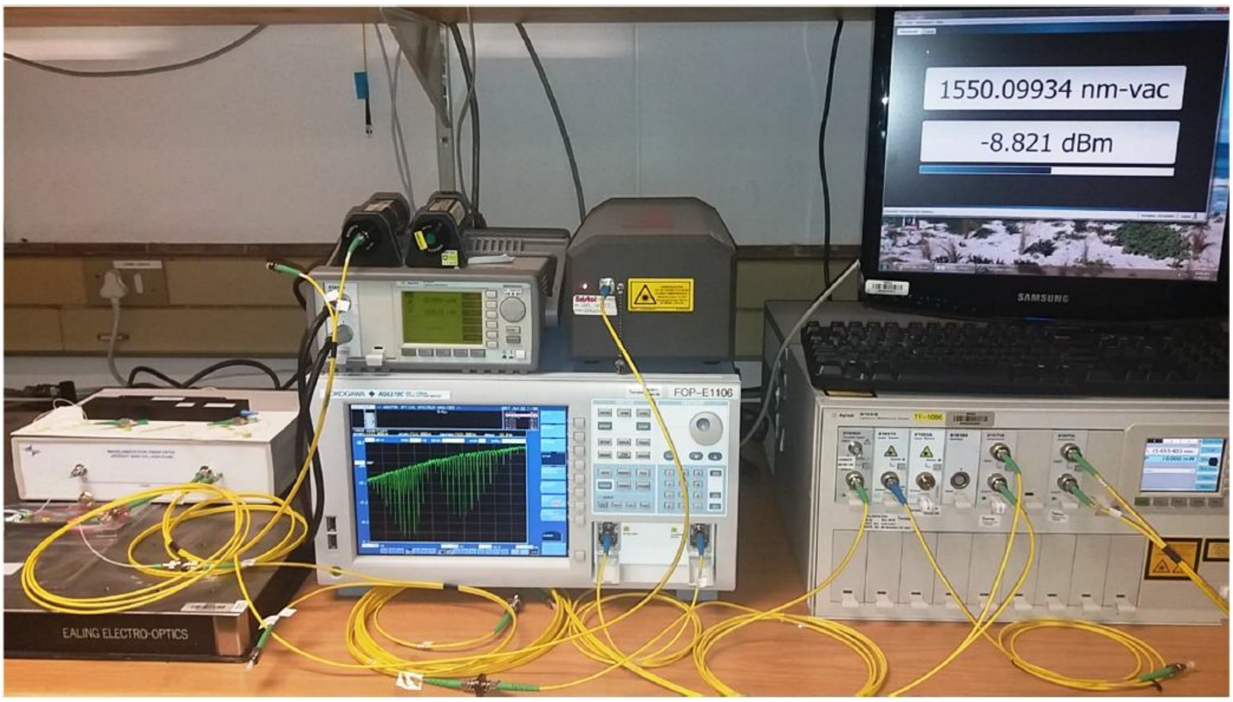

Fig. 5-5 – General view of the NMISA measurement setup

The minimum wavelengths of the selected absorption lines R26, R24, R16, R08, R0, P05, P10, P16, P24, and P26 of the H13C14N gas cell were determined by using measurement procedure with the calibrated Bristol wavelength meter. The tunable laser was swept in 0,0001 nm steps over the expected minimum peak and each time a power measurement was obtained. After each measurement, the minimum power was selected from the table of measurements and the tunable laser adjusted to the corresponding wavelength setting. The laser output wavelength was then measured with the calibrated Bristol wavelength meter. This procedure was performed ten times for each absorption line.

5.3.2 Traceability

NMISA's wavelength traceability comes from a 13C16O gas cell produced by Wavelength References. NMISA calibrated the Bristol wavelength meter, 621A-NIR, by using the 13C16O gas cell. A procedure was followed whereby a few of the absorption lines were selected and measured by stepping 0,0001 nm on the tunable laser and obtaining the minimum power on the power meter for each of the absorption lines respectively.

5.3.3 Results

Table 5-4 – Uncertainty of measurement for the calibrated absorption peaks of the $H^{13}C^{14}N$ gas cell

Source of uncertainty	Estimated uncertainty [nm]	Probability distribution	Standard uncertainty contribution [nm]	Degrees of freedom
Wavelength meter calibration, Calculated combined uncertainty	0,00082	Normal k=2	0,0004119	Infinite
Standard resolution (Wavelength meter)	0,00001	Rectangular $k=\sqrt{3}$	0,000002887	Infinite
Absorption peak roundness Ability to select the minimum point	0,00035	Rectangular $k=\sqrt{3}$	0,000202	Infinite
Temperature effects	0,000	Rectangular $k=\sqrt{3}$	0,000	Infinite
UUT Resolution Tuneable laser wavelength increments	0,0001	Rectangular $k=\sqrt{3}$	0,00005774	Infinite
ESDM (type A)	0,00009	Normal k=1	0,00009	9
Effective Degrees of freedom				Infinite
Combined standard uncertainty Normal			0,00047	
Expanded uncertainty k=2 Level of confidence 95,45%			0,00094	Claimed uncertainty 0,0010 nm

5.4 PTB

5.4.1 Scheme and measurement procedure

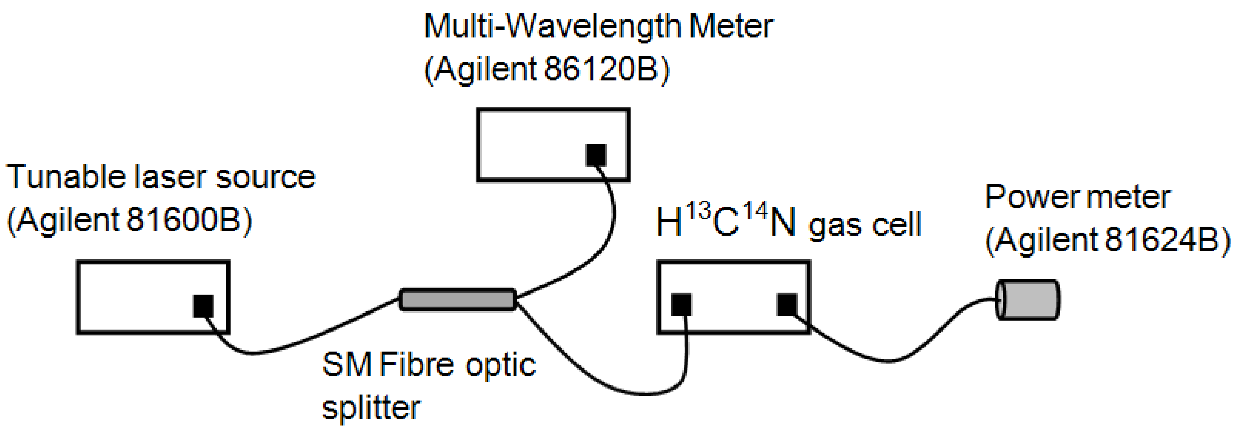

Fig. 5-6 – Setup used for measuring the transmission of the hydrogen cyanide $H^{13}C^{14}N$ reference gas cell within the wavelength range from 1440 nm and 1640 nm.

The centre wavelength of the cell absorption peaks was determined as follows:

The transmitted laser radiation through the cell as a function of the wavelength was measured using the setup shown in Figure 8 by scanning the laser wavelength from 1440 nm to 1640 nm with a low resolution (0.5 nm) to identify the absorption lines of interest.

After identifying a particular absorption line, a high-resolution scan of the line with a resolution of 1 pm was performed and normalized with the laser source spectrum measured with the Multi-Wavelength Meter.

The normalized measurement data are fitted to a double gaussian function:

$$T_{\mathrm{norm}}(\lambda) = 1 - \left(a \cdot e^{-b\cdot(\lambda-c)^2} + d \cdot e^{-e\cdot(\lambda-c)^2}\right)$$

where a, b, c and d are the coefficients to be fitted.

The wavelength centre line of the absorption peak is determined by finding the minimum of the fitted function.

5.4.2 Traceability

The Multi-Wavelength Meter (Agilent 81600B) used for the measurement of the laser wavelengths was calibrated by using reference optical vacuum wavelengths of reference lasers at ref = 813 nm, 1064 nm, 1260 nm, 1299 nm, 1300 nm, 1350 nm, 1370 nm and 1542. The reference laser at 813 nm was a cavity stabilized Ti:sapphire. For the reference wavelengths of 1064 nm and 1542 nm, a Nd:YAG laser and a cavity stabilized fibre laser were respectively used. In the wavelength range from1260 nm to1370 nm, a tunable diode laser was used. During the calibration, the reference wavelengths 813 nm and 1542 nm were measured with a frequency comb referenced to Cs primary standard of PTB [4], while for the wavelength range 1260 nm – 1370 nm a wavemeter of PTB was used.

5.4.3 Results

The uncertainties of the absorption peak wavelengths were determined in accordance with the [2]. As an example, the detailed uncertainty budget for the measurement of the R24 absorption peak is shown in Table 8. The measurand evaluation model is given as,

$$\lambda_{\mathrm{R24}} = \lambda_{\mathrm{Measurement}} \cdot F_{\mathrm{Fitting}} \cdot F_{\mathrm{Background}} \cdot F_{\mathrm{Reproducibility}} \cdot F_{\mathrm{Temperature}} \cdot F_{\mathrm{Repeatability}},$$

where $\lambda_{\mathrm{Measurement}}$ is the wavelength measurement in nm, F_{Fitting}, $F_{\mathrm{Reproducibility}}$, $F_{\mathrm{Temperature}}$ and $F_{\mathrm{Repeatability}}$ are the correction factors associated to the fitting model, background, reproducibility, temperature and repeatability of the measurement, respectively. It should be noted that in this model all correction factors have a value of 1; i.e. the wavelength measurement is not corrected, but the factors uncertainty contributions are considered.

Table 5-5 – Uncertainty budget of the centre wavelength measurement of the R24 absorption peak of the hydrogen cyanide $H^{13}C^{14}N$ reference gas cell.

λ	u_{a1}	u_{b6}	u_{b1}	u_{b2}	u_{b3}	u_s	U_{exp}, pm
	Repeatability	Reproducibility	Wavelength	fitting	Background variations	Summarized	Expanded
R26	0,6003	0,57744	0,606	0,46134	0,020012	1,12887	2,25774
R24	0,6006	0,57776	0,606	0,46160	0,02002	1,129319	2,25863
R16	0,6021	0,57920	0,606	0,46274	0,020072	1,131318	2,26263
R08	0,6039	0,58087	0,606	0,46408	0,020130	1,133646	2,26729
R00	0,6059	0,58278	0,606	0,46560	0,020196	1,136308	2,27261
P05	0,6144	0,59100	0,606	0,47217	0,020481	1,147799	2,29559
P10	0,613	0,5902	0,606	0,47161	0,02045	1,146813	2,29362
P16	0,6109	0,58763	0,606	0,46948	0,020365	1,143087	2,28617
P24	0,6090	0,58579	0,606	0,46801	0,02030	1,140519	2,28103
P26	0,6075	0,58437	0,606	0,46687	0,020252	1,138525	2,2770
distribution	Standard	Rectangular	Standard	Rectangular	Standard	Standard	Standard k=2

Major contributions to the total uncertainty are the uncertainties associated with the wavelength measurement, the repeatability and the reproducibility of the measurement setup as well as the fitting model (mean standard deviation between model fitting and measurements).

5.5 NIS

5.5.1 Scheme and measurement procedure

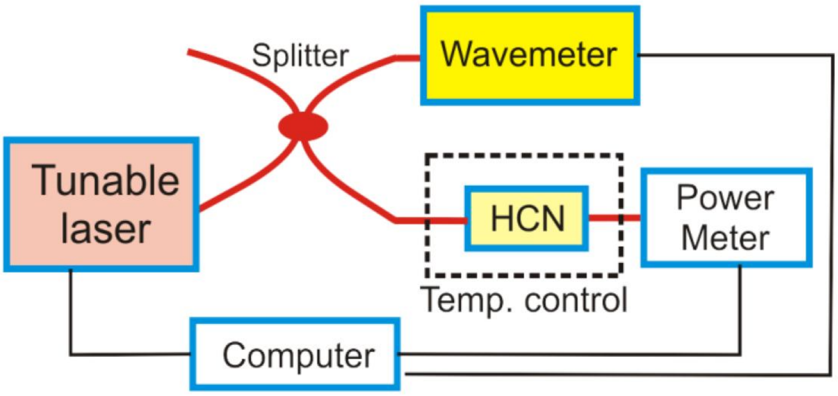

Fig. 5-7 – The system used measure the absorption lines wavelength of the fiber coupled HCN gas cell

A Labview program is developed to allow the laser to scan by steps of 1 pm over only the 10 peaks under consideration in this comparison (R26, R24, R16, R08, R0, P05, P10, P16, P24, and P26). At the same while, the program reads the wavelength of the laser and the power of the passed beam through the HCN cell. The HCN cell is placed in a thermoelectric temperature control box that is controlled with TEC controller. The measurement trace is then processed with origin by fitting the trace with Gaussian fitting of multiple peaks to find the center of the peaks.

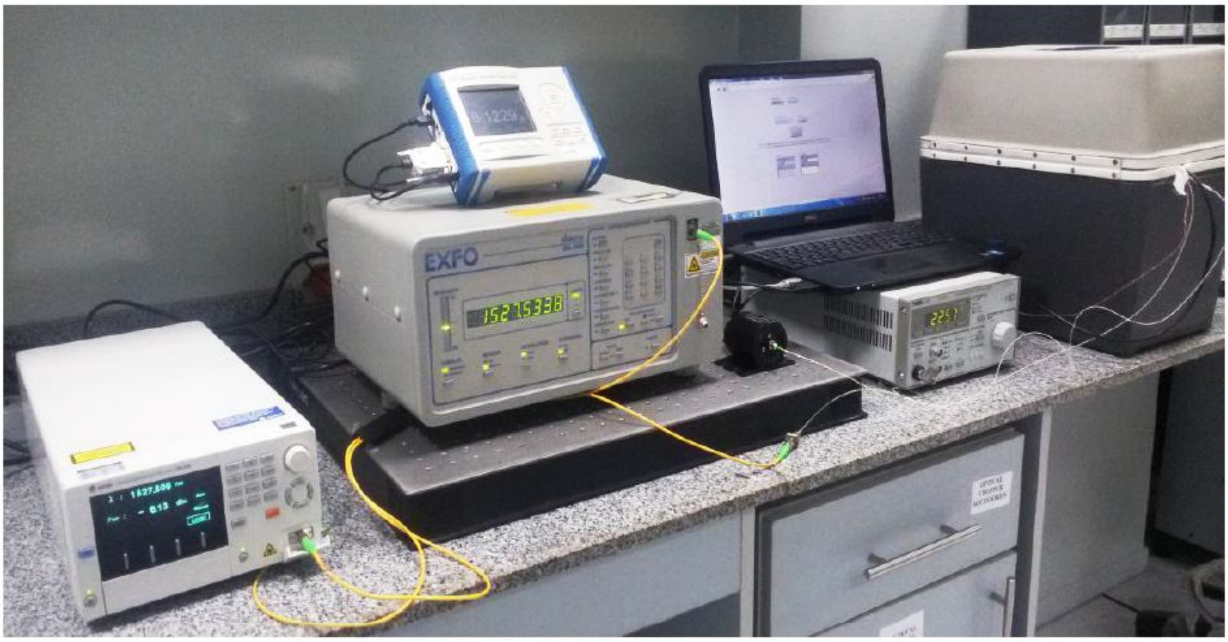

Fig. 5-8 – General view of the setup used for the wavelength of the HCN absorption lines measurements

5.5.2 Traceability

Wavelength measurement: The wavemeter is calibrated using our Primary length standard, which is the Iodine stabilized He-Ne laser near 633 nm (Internationally recognized activity) (traceability to the SI unit of length) [5]. Additionally, it is calibrated using the hyperfine transitions of the two-photon stabilized laser near (778 nm, 1556 nm) [6]. The absolute frequency of the hyperfine components of the two-photon stabilized laser is measured using an optical frequency comb [7]. The optical frequency comb is linked to a frequency standard which is traceable to the SI unit of time and frequency.

5.5.3 Results

Table 5-6 – Uncertainty budget of the wavelength measurement (Example: line P26)

Source of uncertainty	Value	PD	DIV	DOF	Sensitivity Coefficient	Standard Uncertainty
Wavemeter	0,30 pm	Rectangular	√3	∞	1	0,17 pm
Temperature	1 °C	Triangle	√6	∞	0	0 pm
Curve fitting	0,34 pm	Normal	1	400	1	0,34 pm
Repeatability (Reprodu-cibility)	0,10 pm	Normal	1	19	1	0,10 pm
Combined uncertainty			0,39 pm			
Effective degrees of freedom			617			
Expanded uncertainty (k=2)			0,78 pm			

Div: Divisor, DOF: degrees-of-freedom, PD: Probability distribution

Table 5-7 – Final expanded uncertainties of the 10 absorption lines

Wavelength peak	Expanded uncertainty (pm)
R26	0,8
R24	0,5
R16	0,5
R08	0,5
R0	0,6
P05	0,6
P10	0,5
P16	0,5
P24	0,7
P26	0,8

6 Results

All the values and participants uncertainties were agreed and approved by all participants at predraft A preparation stage.

6.1 Transportation drift. Artifact stability.

The artifact stability was checked by the Pilot after the artifact had been returned to the Pilot. So there were two measurements by pilot – before delivering the artifact to participants and after receiving it from the last one.

From the tables 4-2, 4-3 we can see that maximum artifact drift value for all wavelengths is no more than 0.2 pm. The relative drift Δ_{ins} for each wavelength is taken into account as additional relative uncertainty in calculations for each participant (supposed rectangular probability distribution):

$$\Delta_{ins} = \frac{\lambda_1^p - \lambda_2^p}{\lambda_{average}^p}, \qquad (6\text{-}1)$$

where λ_1^p, λ_2^p – the first and the final values of wavelength measured by the Pilot;

$\lambda_{average}^p$ – average value for Pilot measurements.

Table 6-1 – Values of the relative drift Δ_{ins}

Wavelength peak	Δ_{ins}
R26	-6,55E-08
R24	-1,31E-07
R16	1,31E-07
R08	6,51E-08
R00	-1,95E-07
P05	-1,29E-07
P10	-6,45E-08
P16	-1,29E-07
P24	-3,84E-07
P26	1,28E-07

6.2 Difference from Pilot

The relative difference of measurement results between each participant λ_i and the pilot λ_p (calculated from two values of the pilot as average) was defined for each wavelength as:

$$\Delta_i = \frac{\lambda_i}{\lambda_i^p} - 1 \qquad (6\text{-}2)$$

and it's standard relative uncertainty $u(\Delta_i)$ as:

$$u(\Delta_i) = \sqrt{u_r^2(\lambda_i) + u_{r,ad}^2(\lambda_i)}\ , \qquad (6\text{-}3)$$

where $u_r(\lambda_i)$ – the combined standard uncertainty of *i*-participant;

$u_{r,ad}(\lambda_i)$ – the additional uncertainty of the transfer standard due to the artifact instability (drift). This uncertainty is defined as:

$$u_{r,ad}(\lambda_i) = \frac{|\Delta_{ins}|}{2\sqrt{3}}\ , \qquad (6\text{-}4)$$

Δ_{ins} – artifact drift showed in table 6-1.

For the pilot lab (*i*=0), $\Delta_0 = 0$ and the uncertainty $u(\Delta_0)$ are also calculated by (6-3).

The calculated results are summarized in Tables 6-2 – 6-11.

Table 6-2 – Difference of participants results from Pilot and its uncertainty for R26

R26	λ_i, nm	λ_i^P, nm	$u_r(\lambda_i)$	$u_{r,ad}(\lambda_i)$	Δ_i	$u(\Delta_i)$
VNIIOFI	1527,6336	1527,6336	1,98346E-07	1,88969E-08	0	1,99244E-07
BelGIM	1527,6335		7,26614E-08		-1,30921E-08	7,50784E-08
NIM	1527,6335		1,5056E-07		-1,96382E-08	1,51741E-07
NMISA	1527,6335		3,07665E-07		-3,27304E-08	3,08245E-07
PTB	1527,6336		7,38397E-07		3,27304E-08	7,38639E-07
NIS	1527,6336		2,61843E-07		3,27304E-08	2,62524E-07

Table 6-3 – Difference of participants results from Pilot and its uncertainty for R24

R24	λ_i, nm	λ_i^P, nm	$u_r(\lambda_i)$	$u_{r,ad}(\lambda_i)$	Δ_i	$u(\Delta_i)$
VNIIOFI	1528,4859	1528,4859	1,57018E-07	3,77727E-08	0	1,61498E-07
BelGIM	1528,4859		7,85091E-08		-1,96273E-08	8,71232E-08
NIM	1528,4859		1,50476E-07		-1,30848E-08	1,55144E-07
NMISA	1528,4862		3,07494E-07		1,96273E-07	3,09805E-07
PTB	1528,4855		7,38849E-07		-2,61697E-07	7,39814E-07
NIS	1528,4860		1,63561E-07		6,54242E-08	1,67866E-07

Table 6-4 – Difference of participants results from Pilot and its uncertainty for R16

R16	λ_i, nm	λ_i^P, nm	$u_r(\lambda_i)$	$u_{r,ad}(\lambda_i)$	Δ_i	$u(\Delta_i)$
VNIIOFI	1532,2830	1532,2830	1,60218E-07	3,76791E-08	0	1,64589E-07
BelGIM	1532,2832		6,91778E-08		1,10946E-07	7,87736E-08
NIM	1532,2832		1,50103E-07		9,78931E-08	1,5476E-07
NMISA	1532,2830		3,06732E-07		0	3,09037E-07
PTB	1532,2831		7,38322E-07		6,52621E-08	7,39283E-07
NIS	1532,2832		1,63155E-07		1,30524E-07	1,6745E-07

Table 6-5 – Difference of participants results from Pilot and its uncertainty for R08

R08	λ_i, nm	λ_i^P, nm	$u_r(\lambda_i)$	$u_{r,ad}(\lambda_i)$	Δ_i	$u(\Delta_i)$
VNIIOFI	1536,7037	1536,7037	1,56504E-07	1,87853E-08	0	1,57627E-07
BelGIM	1536,7037		8,13429E-08		6,50744E-09	8,34839E-08
NIM	1536,7036		1,49671E-07		-2,60297E-08	1,50845E-07
NMISA	1536,7038		3,05849E-07		9,76115E-08	3,06426E-07
PTB	1536,7033		7,37713E-07		-2,2776E-07	7,37953E-07
NIS	1536,7039		1,62686E-07		1,62686E-07	1,63767E-07

Table 6-6 – Difference of participants results from Pilot and its uncertainty for R00

R00	λ_i, nm	λ_i^P, nm	$u_r(\lambda_i)$	$u_{r,ad}(\lambda_i)$	Δ_i	$u(\Delta_i)$
VNIIOFI	1541,7528	1541,7528	1,62477E-07	5,61715E-08	0	1,71913E-07
BelGIM	1541,7526		7,91307E-08		-9,72919E-08	9,70408E-08
NIM	1541,7526		1,49181E-07		-1,29722E-07	1,59406E-07
NMISA	1541,7528		3,04848E-07		3,24306E-08	3,0998E-07
PTB	1541,7523		7,37024E-07		-2,91876E-07	7,39161E-07
NIS	1541,7528		1,94584E-07		3,24306E-08	2,02529E-07

Table 6-7 – Difference of participants results from Pilot and its uncertainty for P05

P05	λ_i, nm	λ_i^P, nm	$u_r(\lambda_i)$	$u_{r,ad}(\lambda_i)$	Δ_i	$u(\Delta_i)$
VNIIOFI	1545,9558	1545,9558	1,57831E-07	3,73458E-08	0	1,62189E-07
BelGIM	1545,9557		7,24471E-08		-9,70274E-08	8,15064E-08
NIM	1545,9557		1,48775E-07		-7,76219E-08	1,53391E-07
NMISA	1545,9558		3,04019E-07		0	3,06304E-07
PTB	1545,9556		7,42453E-07		-1,2937E-07	7,43392E-07
NIS	1545,9559		1,94055E-07		6,46849E-08	1,97616E-07

Table 6-8 – Difference of participants results from Pilot and its uncertainty for P10

P10	λ_i, nm	λ_i^P, nm	$u_r(\lambda_i)$	$u_{r,ad}(\lambda_i)$	Δ_i	$u(\Delta_i)$
VNIIOFI	1549,7303	1549,7303	1,59705E-07	1,86274E-08	0	1,60788E-07
BelGIM	1549,7304		7,09801E-08		7,74328E-08	7,33836E-08
NIM	1549,7305		1,48413E-07		1,4196E-07	1,49577E-07
NMISA	1549,7306		3,03279E-07		2,25846E-07	3,0385E-07
PTB	1549,7305		7,40009E-07		1,61318E-07	7,40243E-07
NIS	1549,7305		1,61318E-07		1,61318E-07	1,6239E-07

Table 6-9 – Difference of participants results from Pilot and its uncertainty for P16

P16	λ_i, nm	λ_i^P, nm	$u_r(\lambda_i)$	$u_{r,ad}(\lambda_i)$	Δ_i	$u(\Delta_i)$
VNIIOFI	1554,5904	1554,5904	1,57598E-07	3,71384E-08	0	1,61915E-07
BelGIM	1554,5906		7,71907E-08		9,64884E-08	8,56602E-08
NIM	1554,5905		1,47949E-07		8,36233E-08	1,52539E-07
NMISA	1554,5908		3,0233E-07		2,57303E-07	3,04603E-07
PTB	1554,5906		7,35298E-07		1,28651E-07	7,36235E-07
NIS	1554,5907		1,60814E-07		1,92977E-07	1,65047E-07

Table 6-10 – Difference of participants results from Pilot and its uncertainty for P24

P24	λ_i, nm	λ_i^P, nm	$u_r(\lambda_i)$	$u_{r,ad}(\lambda_i)$	Δ_i	$u(\Delta_i)$
VNIIOFI	1561,6355	1561,6355	1,75777E-07	1,10913E-07	0	2,07844E-07
BelGIM	1561,6357		6,78775E-08		1,0886E-07	1,30034E-07
NIM	1561,6357		1,47281E-07		1,0886E-07	1,84373E-07
NMISA	1561,6360		3,00966E-07		3,20177E-07	3,20753E-07
PTB	1561,6359		7,30336E-07		2,56142E-07	7,3871E-07
NIS	1561,6360		2,24124E-07		3,20177E-07	2,50066E-07

Table 6-11 – Difference of participants results from Pilot and its uncertainty for P26

P26	λ_i, nm	λ_i^P, nm	$u_r(\lambda_i)$	$u_{r,ad}(\lambda_i)$	Δ_i	$u(\Delta_i)$
VNIIOFI	1563,4988	1563,4988	1,86121E-07	3,69268E-08	0	1,89749E-07
BelGIM	1563,4984		8,25073E-08		-2,8142E-07	9,03938E-08
NIM	1563,4984		1,47106E-07		-2,68628E-07	1,5167E-07
NMISA	1563,4985		3,00608E-07		-1,91877E-07	3,02867E-07
PTB	1563,4981		7,28191E-07		-4,47714E-07	7,29127E-07
NIS	1563,4985		2,55837E-07		-1,91877E-07	2,58488E-07

6.3 Comparison Reference Value

The CRV (comparison reference value) was calculated according to the Guidelines [1]:

At first, the cut-off value of the uncertainty is determined by:

$$u_{cut-off} = \text{average}\{u_r(\lambda_i)\} \text{ for } u_r(\lambda_i) \le \text{median}\{u_r(\lambda_i)\} \ (i = 0 \text{ to N}), \tag{6-5}$$

where N is the number of participants excluding the pilot (N = 5), pilot is counting as 0.

Then the reported uncertainty of each NMI is adjusted by the cut-off as:

$$\begin{matrix} u_{r,adj}(\lambda_i) = u_r(\lambda_i) \\ u_{r,adj}(\lambda_i) = u_{cut-off} \end{matrix} \ \text{for} \ \begin{matrix} u_r(\lambda_i) \ge u_{cut-off} \\ u_r(\lambda_i) < u_{cut-off} \end{matrix} \ (i = 0 \text{ to } N). \tag{6-6}$$

The uncertainty of the relative difference Δ_i after cut-off is also adjusted by:

$$u_{adj}(\Delta_i) = \sqrt{u_{r,adj}^2(\lambda_i) + u_{r,ad}^2(\lambda_i)} \tag{6-7}$$

The weights w_i are then calculated by [1]:

$$w_i = \frac{u_{adj}^{-2}(\Delta_i)}{\sum_{j=0}^{N} u_{adj}^{-2}(\Delta_j)} \tag{6-8}$$

So the CRV, Δ_{CRV} is determined by

$$\Delta_{\mathrm{CRV}} = \sum_{i=0}^{N} w_i \Delta_i \tag{6-9}$$

and the standard uncertainty of the CRV is given by

$$u(\Delta_{\mathrm{CRV}}) = \frac{\sqrt{\sum_{i=0}^{N} \frac{u^2(\Delta_i)}{u_{adj}^4(\Delta_i)}}}{\sum_{i=0}^{N} u_{adj}^{-2}(\Delta_i)}. \tag{6-10}$$

Then the expanded uncertainty of the CRV is calculated as $U(\Delta_{\mathrm{CRV}}) = k \cdot u(\Delta_{\mathrm{CRV}})$ (k=2).

The calculated values (tentative CRV) are summarized in Table 6-12 – Table 6-22 based on the summarized results in Table 6-2 – Table 6-11.

Table 6-12 – Values $u_{cut-off}$ for each wavelength

Wavelength peak	$u_{cut-off}$	Wavelength peak	$u_{cut-off}$
R26	1,40522E-07	P05	1,26351E-07
R24	1,28668E-07	P10	1,26366E-07
R16	1,26500E-07	P16	1,27579E-07
R08	1,29173E-07	P24	1,30312E-07
R00	1,30263E-07	P26	1,38578E-07

Table 6-13 – CRV and its uncertainty (R26)

R26	VNIIOFI	BelGIM	NIM	NMISA	PTB	NIS
Δ_i	0,00	-1,30921E-08	-1,96382E-08	-3,27304E-08	3,27304E-08	3,27304E-08
$u(\Delta_i)$	1,99244E-07	7,50784E-08	1,51741E-07	3,08245E-07	7,38639E-07	2,62524E-07
$u_{r,adj}(\lambda_i)$	1,98346E-07	1,70852E-07	1,70852E-07	3,07665E-07	7,38397E-07	2,61843E-07
$u_{adj}(\Delta_i)$	1,99244E-07	1,71894E-07	1,71894E-07	3,08245E-07	7,38639E-07	2,62524E-07
w_i	0,173	0,343	0,299	0,072	0,013	0,100
Δ_{CRV}	-9,04566E-09					
$u(\Delta_{\mathrm{CRV}})$	7,20313E-08					

Table 6-14 – CRV and its uncertainty (R24)

R24	VNIIOFI	BelGIM	NIM	NMISA	PTB	NIS
Δ_i	0,00	-1,96273E-08	-1,30848E-08	1,96273E-07	-2,61697E-07	6,54242E-08
$u(\Delta_i)$	1,61498E-07	8,71232E-08	1,55144E-07	3,09805E-07	7,39814E-07	1,67866E-07
$u_{r,adj}(\lambda_i)$	1,57018E-07	1,28668E-07	1,50476E-07	3,07494E-07	7,38849E-07	1,63561E-07
$u_{adj}(\Delta_i)$	1,61498E-07	1,34097E-07	1,55144E-07	3,09805E-07	7,39814E-07	1,67866E-07
w_i	0,209	0,303	0,227	0,057	0,010	0,194
Δ_{CRV}	1,22984E-08					
$u(\Delta_{\mathrm{CRV}})$	6,70848E-08					

Table 6-15 – CRV and its uncertainty (R16)

R16	VNIIOFI	BelGIM	NIM	NMISA	PTB	NIS
Δ_i	0,00	1,10946E-07	9,78931E-08	0,00000E+00	6,52621E-08	1,30524E-07
$u(\Delta_i)$	1,64589E-07	7,87736E-08	1,54760E-07	3,09037E-07	7,39283E-07	1,67450E-07
$u_{r,adj}(\lambda_i)$	1,60218E-07	1,26500E-07	1,50103E-07	3,06732E-07	7,38322E-07	1,63155E-07
$u_{adj}(\Delta_i)$	1,64589E-07	1,31992E-07	1,54760E-07	3,09037E-07	7,39283E-07	1,67450E-07
w_i	0,201	0,312	0,227	0,057	0,010	0,194
Δ_{CRV}	8,27574E-08					
$u(\Delta_{\mathrm{CRV}})$	6,58992E-08					

Table 6-16 – CRV and its uncertainty (R08)

R08	VNIIOFI	BelGIM	NIM	NMISA	PTB	NIS
Δ_i	0,00	6,50744E-09	-2,60297E-08	9,76115E-08	-2,27760E-07	1,62686E-07
$u(\Delta_i)$	1,57627E-07	8,34839E-08	1,50845E-07	3,06426E-07	7,37953E-07	1,63767E-07
$u_{r,adj}(\lambda_i)$	1,56504E-07	1,29173E-07	1,49671E-07	3,05849E-07	7,37713E-07	1,62686E-07
$u_{adj}(\Delta_i)$	1,57627E-07	1,30531E-07	1,50845E-07	3,06426E-07	7,37953E-07	1,63767E-07
w_i	0,209	0,305	0,228	0,055	0,010	0,194
Δ_{CRV}	3,07552E-08					
$u(\Delta_{\mathrm{CRV}})$	6,52388E-08					

Table 6-17 – CRV and its uncertainty (R00)

R00	VNIIOFI	BelGIM	NIM	NMISA	PTB	NIS
Δ_i	0,00	-9,72919E-08	-1,29722E-07	3,24306E-08	-2,91876E-07	3,24306E-08
$u(\Delta_i)$	1,71913E-07	9,70408E-08	1,59406E-07	3,09980E-07	7,39161E-07	2,02529E-07
$u_{r,adj}(\lambda_i)$	1,62477E-07	1,30263E-07	1,49181E-07	3,04848E-07	7,37024E-07	1,94584E-07
$u_{adj}(\Delta_i)$	1,71913E-07	1,41858E-07	1,59406E-07	3,09980E-07	7,39161E-07	2,02529E-07
w_i	0,212	0,312	0,247	0,065	0,011	0,153
Δ_{CRV}	-5,85949E-08					
$u(\Delta_{\mathrm{CRV}})$	7,2321E-08					

Table 6-18 – CRV and its uncertainty (P05)

P05	VNIIOFI	BelGIM	NIM	NMISA	PTB	NIS
Δ_i	0,00	-9,70274E-08	-7,76219E-08	0,00000E+00	-1,29370E-07	6,46849E-08
$u(\Delta_i)$	1,62189E-07	8,15064E-08	1,53391E-07	3,06304E-07	7,43392E-07	1,97616E-07
$u_{r,adj}(\lambda_i)$	1,57831E-07	1,26351E-07	1,48775E-07	3,04019E-07	7,42453E-07	1,94055E-07
$u_{adj}(\Delta_i)$	1,62189E-07	1,31755E-07	1,53391E-07	3,06304E-07	7,43392E-07	1,97616E-07
w_i	0,216	0,327	0,241	0,060	0,010	0,145
Δ_{CRV}	-4,23735E-08					
$u(\Delta_{\mathrm{CRV}})$	6,73055E-08					

Table 6-19 – CRV and its uncertainty (P10)

P10	VNIIOFI	BelGIM	NIM	NMISA	PTB	NIS
Δ_i	0,00	7,74328E-08	1,41960E-07	2,25846E-07	1,61318E-07	1,61318E-07
$u(\Delta_i)$	1,60788E-07	7,33836E-08	1,49577E-07	3,03850E-07	7,40243E-07	1,62390E-07
$u_{r,adj}(\lambda_i)$	1,59705E-07	1,26366E-07	1,48413E-07	3,03279E-07	7,40009E-07	1,61318E-07
$u_{adj}(\Delta_i)$	1,60788E-07	1,27732E-07	1,49577E-07	3,03850E-07	7,40243E-07	1,62390E-07
w_i	0,198	0,314	0,229	0,055	0,009	0,194
Δ_{CRV}	1,02174E-07					
$u(\Delta_{\mathrm{CRV}})$	6,35973E-08					

Table 6-20 – CRV and its uncertainty (P16)

P16	VNIIOFI	BelGIM	NIM	NMISA	PTB	NIS
Δ_i	0,00	9,64884E-08	8,36233E-08	2,57303E-07	1,28651E-07	1,92977E-07
$u(\Delta_i)$	1,61915E-07	8,56602E-08	1,52539E-07	3,04603E-07	7,36235E-07	1,65047E-07
$u_{r,adj}(\lambda_i)$	1,57598E-07	1,27579E-07	1,47949E-07	3,02330E-07	7,35298E-07	1,60814E-07
$u_{adj}(\Delta_i)$	1,61915E-07	1,32875E-07	1,52539E-07	3,04603E-07	7,36235E-07	1,65047E-07
w_i	0,204	0,303	0,230	0,058	0,010	0,196
Δ_{CRV}	1,02375E-07					
$u(\Delta_{\mathrm{CRV}})$	6,63274E-08					

Table 6-21 – CRV and its uncertainty (P24)

P24	VNIIOFI	BelGIM	NIM	NMISA	PTB	NIS
Δ_i	0,00	1,08860E-07	1,08860E-07	3,20177E-07	2,56142E-07	3,20177E-07
$u(\Delta_i)$	2,07844E-07	1,30034E-07	1,84373E-07	3,20753E-07	7,38710E-07	2,50066E-07
$u_{r,adj}(\lambda_i)$	1,75777E-07	1,30312E-07	1,47281E-07	3,00966E-07	7,30336E-07	2,24124E-07
$u_{adj}(\Delta_i)$	2,07844E-07	1,71122E-07	1,84373E-07	3,20753E-07	7,38710E-07	2,50066E-07
w_i	0,203	0,299	0,257	0,085	0,016	0,140
Δ_{CRV}	1,36719E-07					
$u(\Delta_{\mathrm{CRV}})$	8,74452E-08					

Table 6-22 – CRV and its uncertainty (P26)

P26	VNIIOFI	BelGIM	NIM	NMISA	PTB	NIS
Δ_i	0,00	-2,81420E-07	-2,68628E-07	-1,91877E-07	-4,47714E-07	-1,91877E-07
$u(\Delta_i)$	1,89749E-07	9,03938E-08	1,51670E-07	3,02867E-07	7,29127E-07	2,58488E-07
$u_{r,adj}(\lambda_i)$	1,86121E-07	1,38578E-07	1,47106E-07	3,00608E-07	7,28191E-07	2,55837E-07
$u_{adj}(\Delta_i)$	1,89749E-07	1,43414E-07	1,51670E-07	3,02867E-07	7,29127E-07	2,58488E-07
w_i	0,188	0,329	0,294	0,074	0,013	0,101
Δ_{CRV}	-2,07310E-07					
$u(\Delta_{CRV})$	8,40624E-08					

6.4 Chi-square Value

To determine the consistency of comparisons results the Chi-square value χ^2_{obs} was calculated according to [1]:

$$\chi^2_{obs} = \sum_{i=0}^{N} \frac{(\Delta_i - \Delta_{CRV})^2}{u^2_{adj}(\Delta_i)} \qquad (6\text{-}11)$$

The calculated values are presented in Table 6-23.

Table 6-23 – Chi-square values

Wavelength peak	χ^2_{obs}	$\chi^2_{0.05}(\nu)$	Consistency $\chi^2_{obs} \le \chi^2_{0.05}(\nu)$
R26	0,04217	11,07049	Satisfied
R24	0,67922	11,07049	Satisfied
R16	0,46164	11,07049	Satisfied
R08	1,03360	11,07049	Satisfied
R00	0,77752	11,07049	Satisfied
P05	0,61946	11,07049	Satisfied
P10	0,81677	11,07049	Satisfied
P16	0,97816	11,07049	Satisfied
P24	1,37353	11,07049	Satisfied
P26	1,73902	11,07049	Satisfied

$\chi^2_{0.05}$ is determined from the table 6-24, $\nu = N\text{-}1=5$.

Table 6-24 – Chi-square value

$\nu = N-1$	$\alpha = 0,05$
1	3,8415
2	5,9915
3	7,8147
4	9,4877
5	11,0705
6	12,5916
7	14,0671
8	15,5073
9	16,9189
10	18,3070

Therefore the consistency is confirmed for all wavelengths and for all participants.

6.5 Degree of Equivalence

The unilateral degree of equivalence (DoE) D_i of the participant *i* is defined by

$$D_i = \Delta_i - \Delta_{CRV} \tag{6-12}$$

and the uncertainty of DoE U_i is given by

$$U_i = k\sqrt{u^2(\Delta_\mathrm{i}) + u^2(\Delta_{CRV}) - 2\cdot\left(\frac{u^2(\Delta_\mathrm{i})}{u_{adj}^2(\Delta_\mathrm{i})} \bigg/ \sum_{i=0}^{N} u_{adj}^{-2}(\Delta_\mathrm{i}) \right)} \tag{6-13}$$

with the coverage factor *k=2* at the level of confidence of approximately 95 %.

Tables 6-25 – 6-34 summarize the calculation results and they are plotted in Fig. 6-3 – 6-12.

Table 6-25 – The relative unilateral degree of equivalence and its uncertainty of each participant for R26.

R26	VNIIOFI	BelGIM	NIM	NMISA	PTB	NIS
Δ_i	0	-1,30921E-08	-1,96382E-08	-3,27304E-08	3,27304E-08	3,27304E-08
Δ_{CRV}	-9,04566E-09	-9,04566E-09	-9,04566E-09	-9,04566E-09	-9,04566E-09	-9,04566E-09
D_i	9,04566E-09	-4,04649E-09	-1,05926E-08	-2,36847E-08	4,17760E-08	4,17760E-08
$u(\Delta_i)$	1,99244E-07	7,50784E-08	1,51741E-07	3,08245E-07	7,38639E-07	2,62524E-07
$u_{adj}(\Delta_i)$	1,99244E-07	1,41787E-07	1,51741E-07	3,08245E-07	7,38639E-07	2,62524E-07
$u(\Delta_{CRV})$	7,20313E-08	7,20313E-08	7,20313E-08	7,20313E-08	7,20313E-08	7,20313E-08
U_i	3,52792E-07	1,66901E-07	2,40354E-07	5,87988E-07	1,46561E-06	4,91268E-07

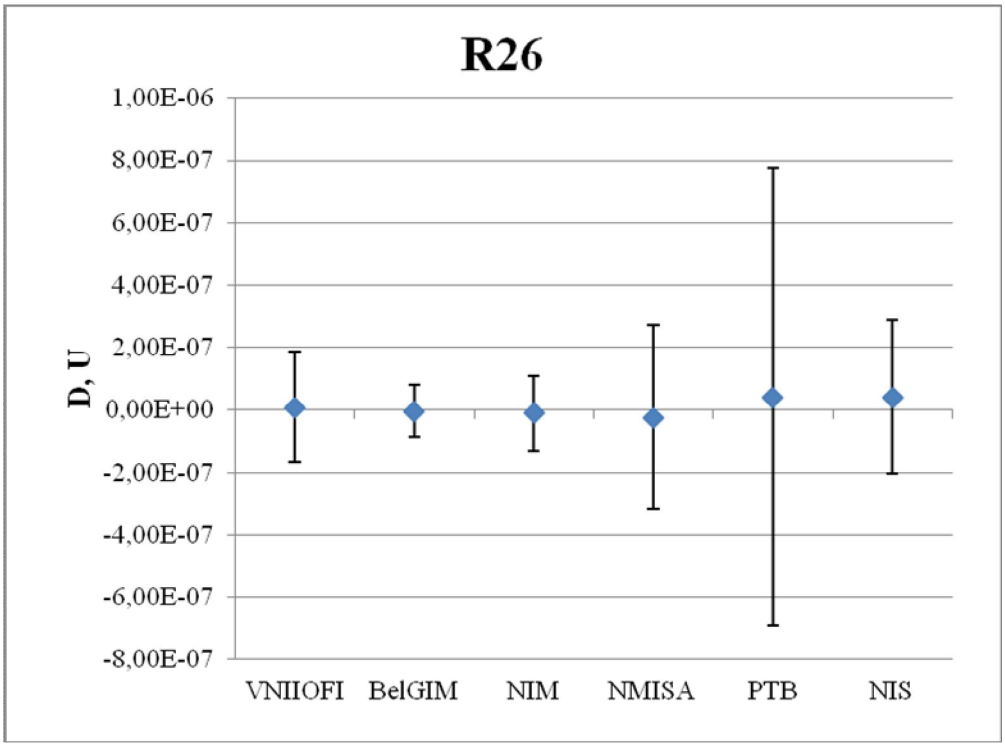

Fig. 6-3 – Relative deviation of the wavelength R26 from the CRV and combined standard uncertainties of participants.

Table 6-26 – The relative unilateral degree of equivalence and its uncertainty of each participant for R24.

R24	VNIIOFI	BelGIM	NIM	NMISA	PTB	NIS
Δ_i	0	-1,96273E-08	-1,30848E-08	1,96273E-07	-2,61697E-07	6,54242E-08
Δ_{CRV}	1,22984E-08	1,22984E-08	1,22984E-08	1,22984E-08	1,22984E-08	1,22984E-08
D_i	-1,22984E-08	-3,19256E-08	-2,53832E-08	1,83974E-07	-2,73995E-07	5,31258E-08
$u(\Delta_i)$	1,61498E-07	8,71232E-08	1,55144E-07	3,09805E-07	7,39814E-07	1,67866E-07
$u_{adj}(\Delta_i)$	1,61498E-07	1,34097E-07	1,55144E-07	3,09805E-07	7,39814E-07	1,67866E-07
$u(\Delta_{CRV})$	6,70848E-08	6,70848E-08	6,70848E-08	6,70848E-08	6,70848E-08	6,70848E-08
U_i	2,80476E-07	1,73014E-07	2,65744E-07	5,98546E-07	1,47093E-06	2,95053E-07

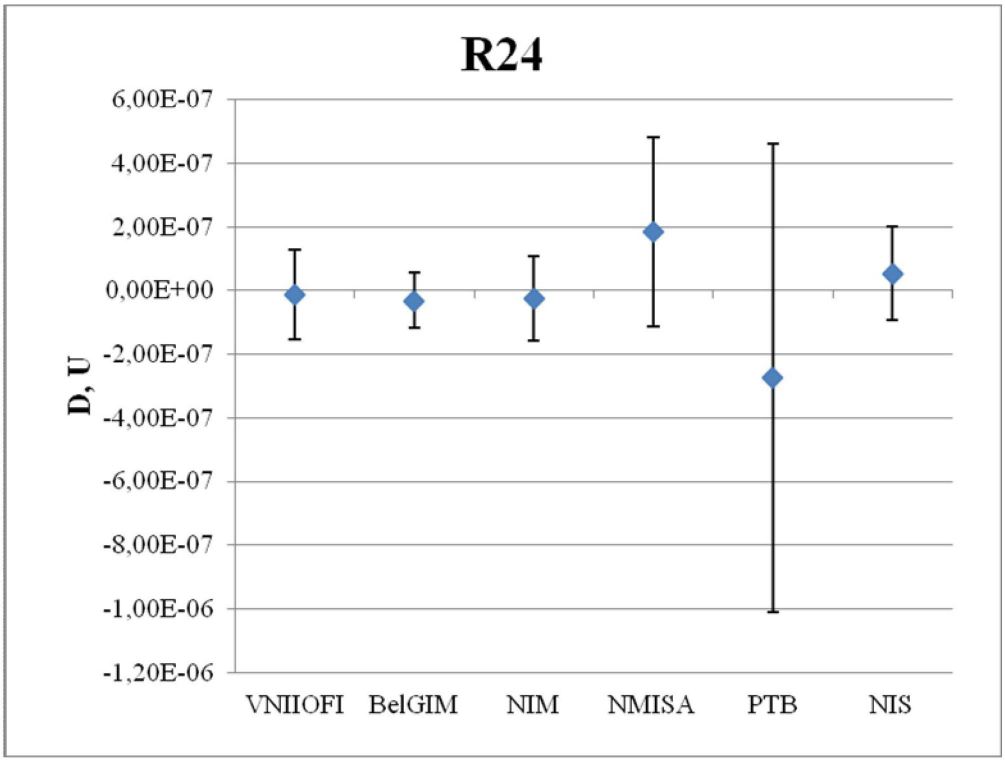

Fig. 6-4 – Relative deviation of the wavelength R24 from the CRV and combined standard uncertainties of participants

Table 6-27 – The relative unilateral degree of equivalence and its uncertainty of each participant for R16.

R16	VNIIOFI	BelGIM	NIM	NMISA	PTB	NIS
Δ_i	0	1,10946E-07	9,78931E-08	0	6,52621E-08	1,30524E-07
Δ_{CRV}	8,27574E-08	8,27574E-08	8,27574E-08	8,27574E-08	8,27574E-08	8,27574E-08
D_i	-8,27574E-08	2,81881E-08	1,51357E-08	-8,27574E-08	-1,74954E-08	4,77667E-08
$u(\Delta_i)$	-1,64589E-07	-7,87736E-08	-1,54760E-07	-3,09037E-07	-7,39283E-07	-1,67450E-07
$u_{adj}(\Delta_i)$	1,64589E-07	1,31992E-07	1,54760E-07	3,09037E-07	7,39283E-07	1,67450E-07
$u(\Delta_{CRV})$	6,58992E-08	6,58992E-08	6,58992E-08	6,58992E-08	6,58992E-08	6,58992E-08
U_i	2,86807E-07	1,63428E-07	2,64012E-07	5,96587E-07	1,46971E-06	2,93355E-07

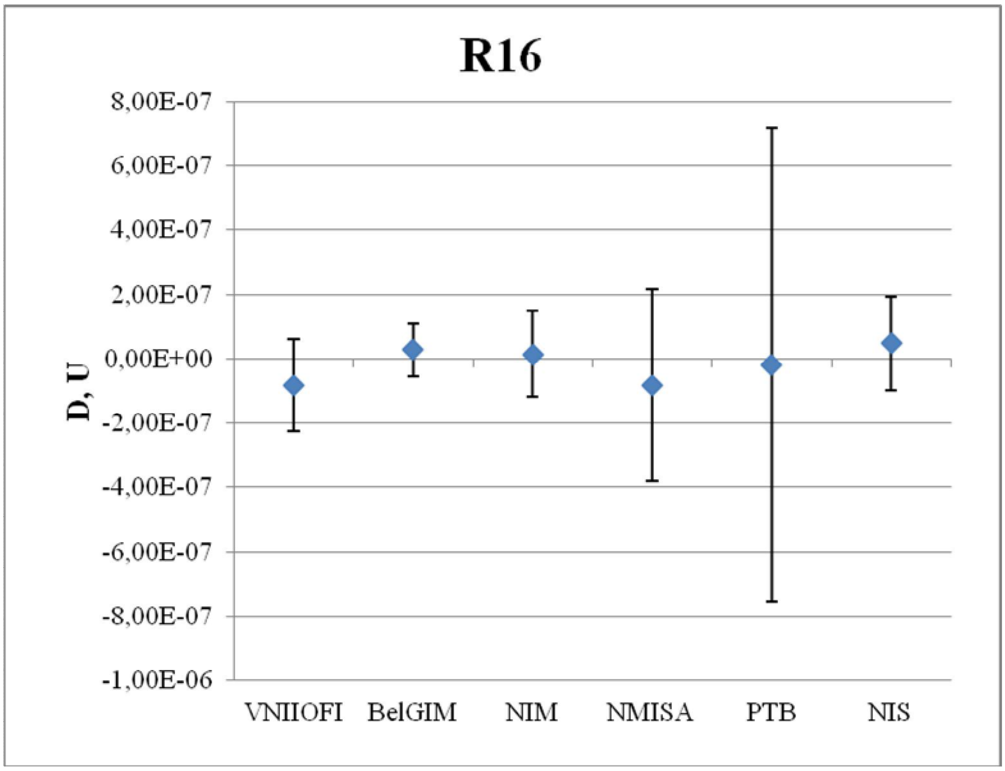

Fig. 6-5 – Relative deviation of the wavelength R16 from the CRV and combined standard uncertainties of participants.

Table 6-28 – The relative unilateral degree of equivalence and its uncertainty of each participant for R08.

R08	VNIIOFI	BelGIM	NIM	NMISA	PTB	NIS
Δ_i	0	6,50744E-09	-2,60297E-08	9,76115E-08	-2,2776E-07	1,62686E-07
Δ_{CRV}	3,07552E-08	3,07552E-08	3,07552E-08	3,07552E-08	3,07552E-08	3,07552E-08
D_i	-3,07552E-08	-2,42477E-08	-5,67849E-08	6,68564E-08	-2,58515E-07	1,31931E-07
$u(\Delta_i)$	1,57627E-07	8,34839E-08	1,50845E-07	3,06426E-07	7,37953E-07	1,63767E-07
$u_{adj}(\Delta_i)$	1,57627E-07	1,30531E-07	1,50845E-07	3,06426E-07	7,37953E-07	1,63767E-07
$u(\Delta_{CRV})$	6,52388E-08	6,52388E-08	6,52388E-08	6,52388E-08	6,52388E-08	6,52388E-08
U_i	2,73652E-07	1,67084E-07	2,57910E-07	5,92526E-07	1,46758E-06	2,87712E-07

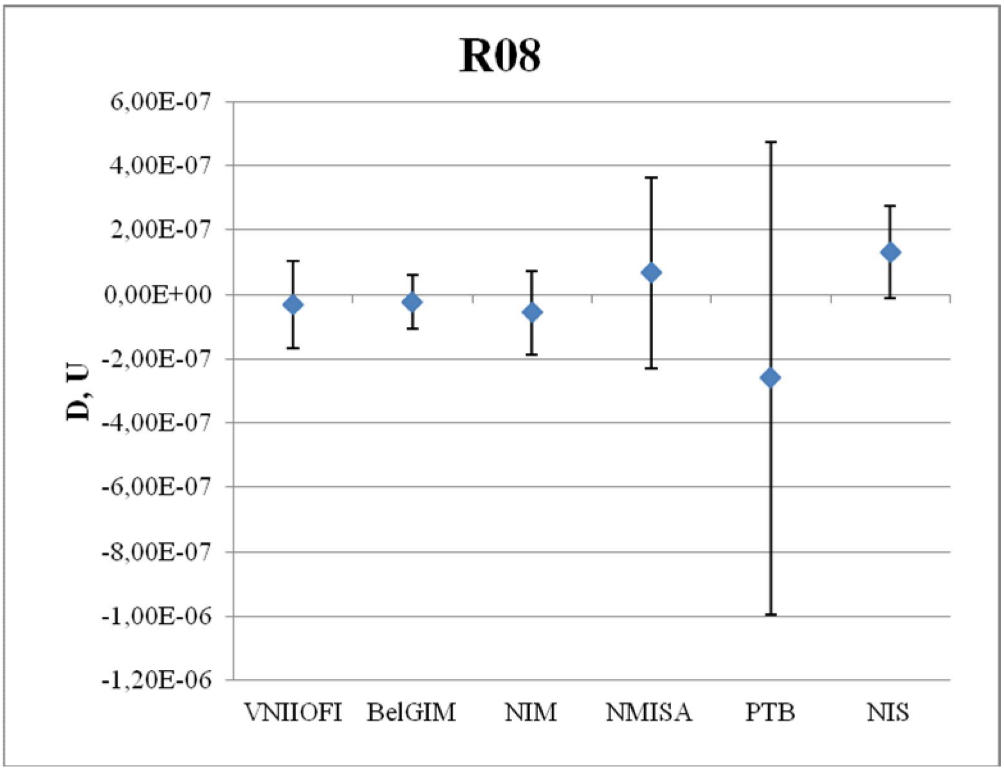

Fig. 6-6 – Relative deviation of the wavelength R08from the CRV and combined standard uncertainties of participants.

Table 6-29 – The relative unilateral degree of equivalence and its uncertainty of each participant for R00.

R00	VNIIOFI	BelGIM	NIM	NMISA	PTB	NIS
Δ_i	0	-9,72919E-08	-1,29722E-07	3,24306E-08	-2,91876E-07	3,24306E-08
Δ_{CRV}	-5,85949E-08	-5,85949E-08	-5,85949E-08	-5,85949E-08	-5,85949E-08	-5,85949E-08
D_i	5,85949E-08	-3,86970E-08	-7,11276E-08	9,10255E-08	-2,33281E-07	9,10255E-08
$u(\Delta_i)$	1,71913E-07	9,70408E-08	1,59406E-07	3,09980E-07	7,39161E-07	2,02529E-07
$u_{adj}(\Delta_i)$	1,71913E-07	1,41858E-07	1,59406E-07	3,09980E-07	7,39161E-07	2,02529E-07
$u(\Delta_{CRV})$	7,23210E-08	7,23210E-08	7,23210E-08	7,23210E-08	7,23210E-08	7,23210E-08
U_i	2,98297E-07	1,87398E-07	2,69082E-07	5,95915E-07	1,46840E-06	3,67201E-07

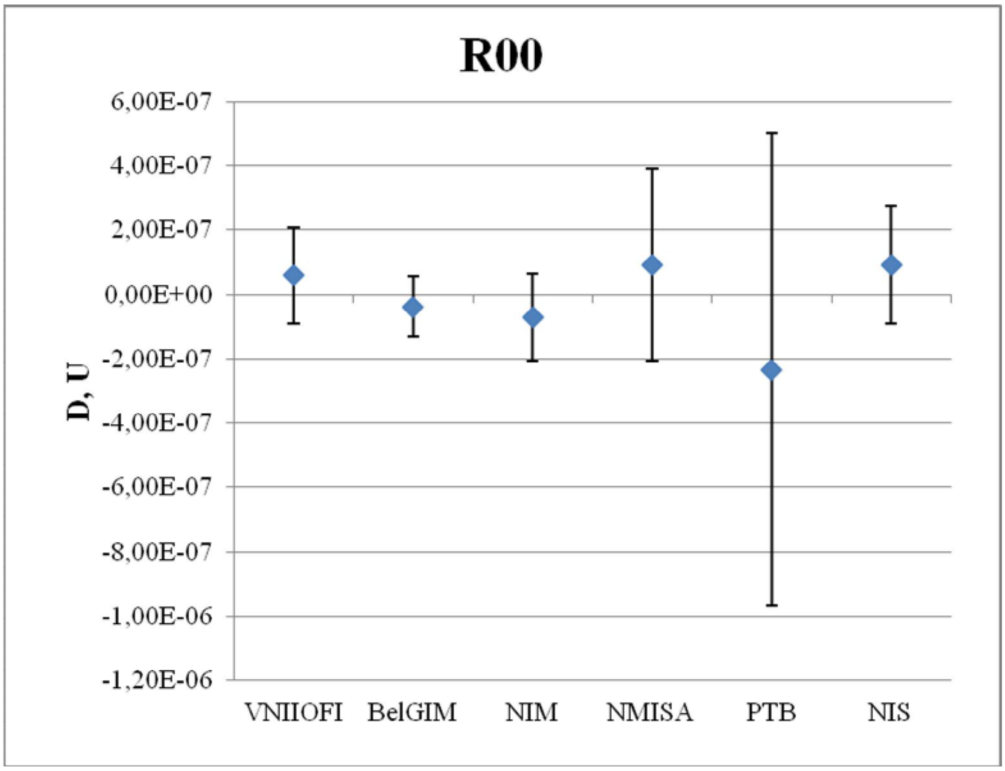

Fig. 6-7 – Relative deviation of the wavelength R00 from the CRV and combined standard uncertainties of participants.

Table 6-30 –The relative unilateral degree of equivalence and its uncertainty of each participant for P05.

P05	VNIIOFI	BelGIM	NIM	NMISA	PTB	NIS
Δ_i	0	-9,70274E-08	-7,76219E-08	0	-1,2937E-07	6,46849E-08
Δ_{CRV}	-4,23735E-08	-4,23735E-08	-4,23735E-08	-4,23735E-08	-4,23735E-08	-4,23735E-08
D_i	4,23735E-08	-5,46539E-08	-3,52484E-08	4,23735E-08	-8,69963E-08	1,07058E-07
$u(\Delta_i)$	1,62189E-07	8,15064E-08	1,53391E-07	3,06304E-07	7,43392E-07	1,97616E-07
$u_{adj}(\Delta_i)$	1,62189E-07	1,31755E-07	1,53391E-07	3,06304E-07	7,43392E-07	1,97616E-07
$u(\Delta_{\mathrm{CRV}})$	6,73055E-08	6,73055E-08	6,73055E-08	6,73055E-08	6,73055E-08	6,73055E-08
U_i	2,79174E-07	1,65280E-07	2,58518E-07	5,89920E-07	1,47758E-06	3,59060E-07

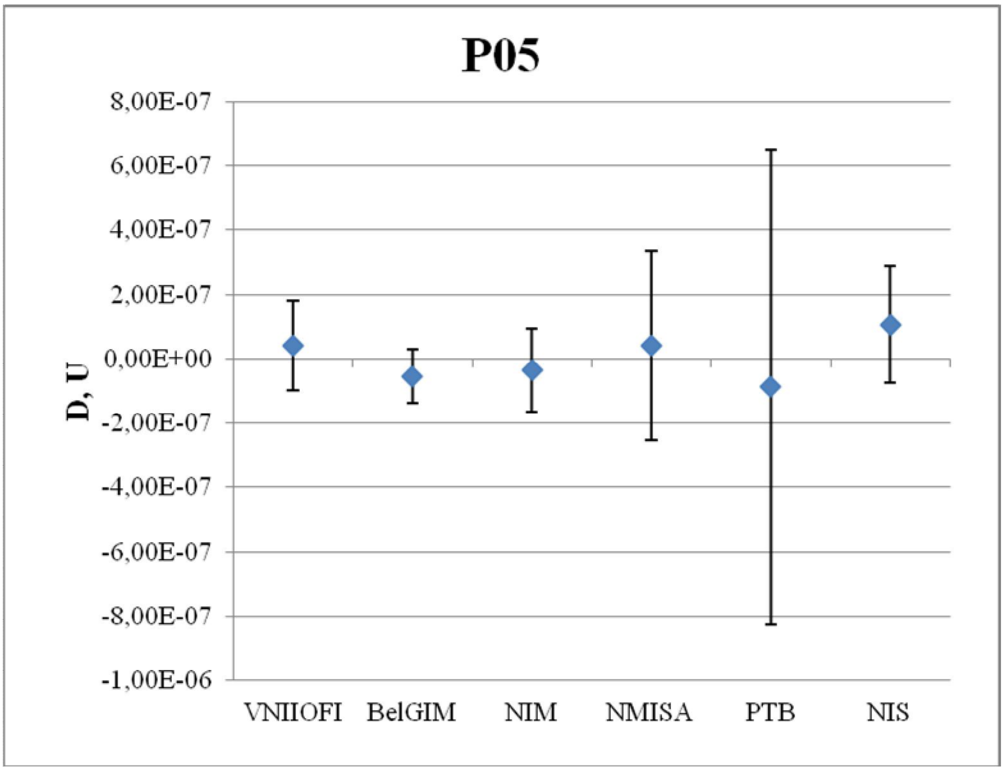

Fig. 6-8 – Relative deviation of the wavelength P05 from the CRV and combined standard uncertainties of participants.

Table 6-31 – The relative unilateral degree of equivalence and its uncertainty of each participant for P10.

P10	VNIIOFI	BelGIM	NIM	NMISA	PTB	NIS
Δ_i	0	7,74328E-08	1,4196E-07	2,25846E-07	1,61318E-07	1,61318E-07
Δ_{CRV}	1,02174E-07	1,02174E-07	1,02174E-07	1,02174E-07	1,02174E-07	1,02174E-07
D_i	-1,02174E-07	-2,47410E-08	3,97863E-08	1,23672E-07	5,91445E-08	5,91445E-08
$u(\Delta_i)$	1,60788E-07	7,33836E-08	1,49577E-07	3,03850E-07	7,40243E-07	1,62390E-07
$u_{adj}(\Delta_i)$	1,60788E-07	1,27732E-07	1,49577E-07	3,03850E-07	7,40243E-07	1,62390E-07
$u(\Delta_{CRV})$	6,35973E-08	6,35973E-08	6,35973E-08	6,35973E-08	6,35973E-08	6,35973E-08
U_i	2,80384E-07	1,55547E-07	2,54358E-07	5,86944E-07	1,47209E-06	2,84054E-07

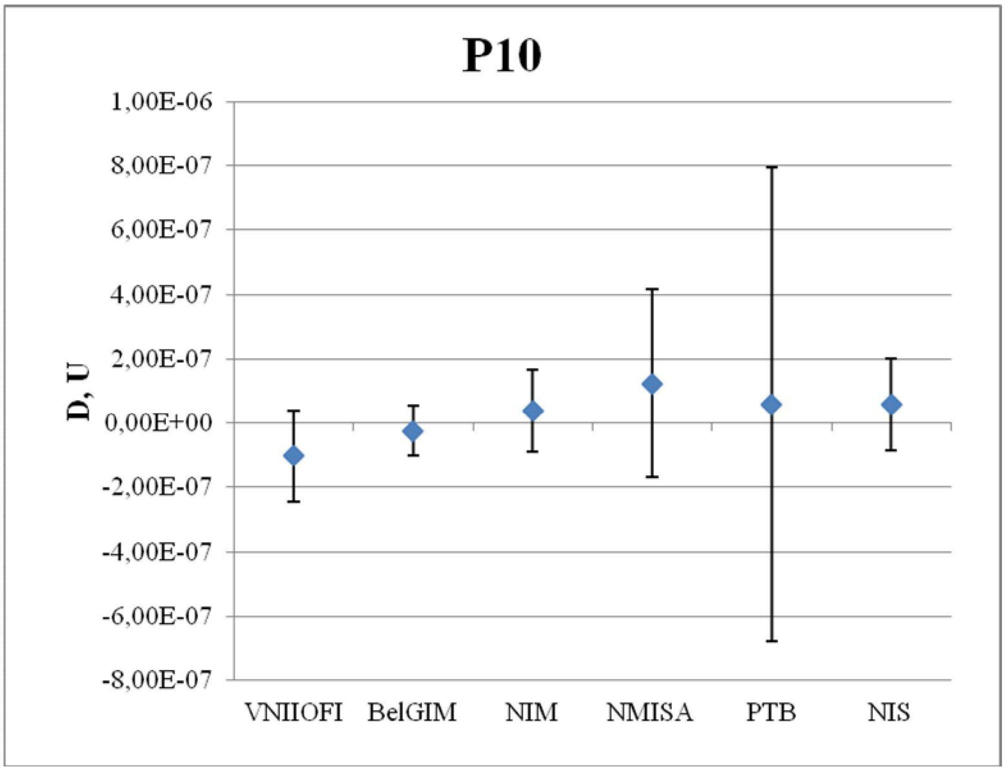

Fig. 6-9 – Relative deviation of the wavelength P10 from the CRV and combined standard uncertainties of participants.

Table 6-32 – The relative unilateral degree of equivalence and its uncertainty of each participant for P16.

P16	VNIIOFI	BelGIM	NIM	NMISA	PTB	NIS
Δ_i	0	9,64884E-08	8,36233E-08	2,57303E-07	1,28651E-07	1,92977E-07
Δ_{CRV}	1,02375E-07	1,02375E-07	1,02375E-07	1,02375E-07	1,02375E-07	1,02375E-07
D_i	-1,02375E-07	-5,88633E-09	-1,87515E-08	1,54928E-07	2,62765E-08	9,06021E-08
$u(\Delta_i)$	1,61915E-07	8,56602E-08	1,52539E-07	3,04603E-07	7,36235E-07	1,65047E-07
$u_{adj}(\Delta_i)$	1,61915E-07	1,32875E-07	1,52539E-07	3,04603E-07	7,36235E-07	1,65047E-07
$u(\Delta_{CRV})$	6,63274E-08	6,63274E-08	6,63274E-08	6,63274E-08	6,63274E-08	6,63274E-08
U_i	2,82317E-07	1,70813E-07	2,60596E-07	5,88192E-07	1,46390E-06	2,89481E-07

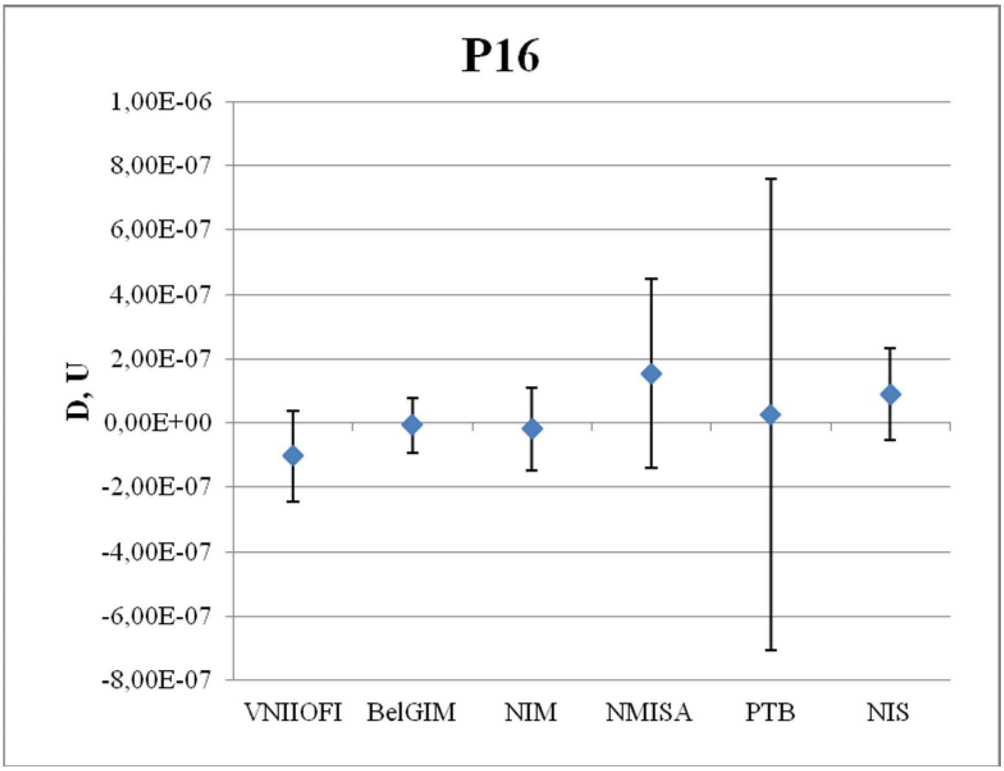

Fig. 6-10 – Relative deviation of the wavelength P16 from the CRV and combined standard uncertainties of participants.

Table 6-33 – The relative unilateral degree of equivalence and its uncertainty of each participant for P24.

P24	VNIIOFI	BelGIM	NIM	NMISA	PTB	NIS
Δ_i	0	1,0886E-07	1,0886E-07	3,20177E-07	2,56142E-07	3,20177E-07
Δ_{CRV}	1,36719E-07	1,36719E-07	1,36719E-07	1,36719E-07	1,36719E-07	1,36719E-07
D_i	-1,36719E-07	-2,78593E-08	-2,78593E-08	1,83458E-07	1,19422E-07	1,83458E-07
$u(\Delta_i)$	2,07844E-07	1,30034E-07	1,84373E-07	3,20753E-07	7,38710E-07	2,50066E-07
$u_{adj}(\Delta_i)$	2,07844E-07	1,71122E-07	1,84373E-07	3,20753E-07	7,38710E-07	2,50066E-07
$u(\Delta_{CRV})$	8,74452E-08	8,74452E-08	8,74452E-08	8,74452E-08	8,74452E-08	8,74452E-08
U_i	3,65195E-07	2,40401E-07	3,10716E-07	6,10000E-07	1,46402E-06	4,59024E-07

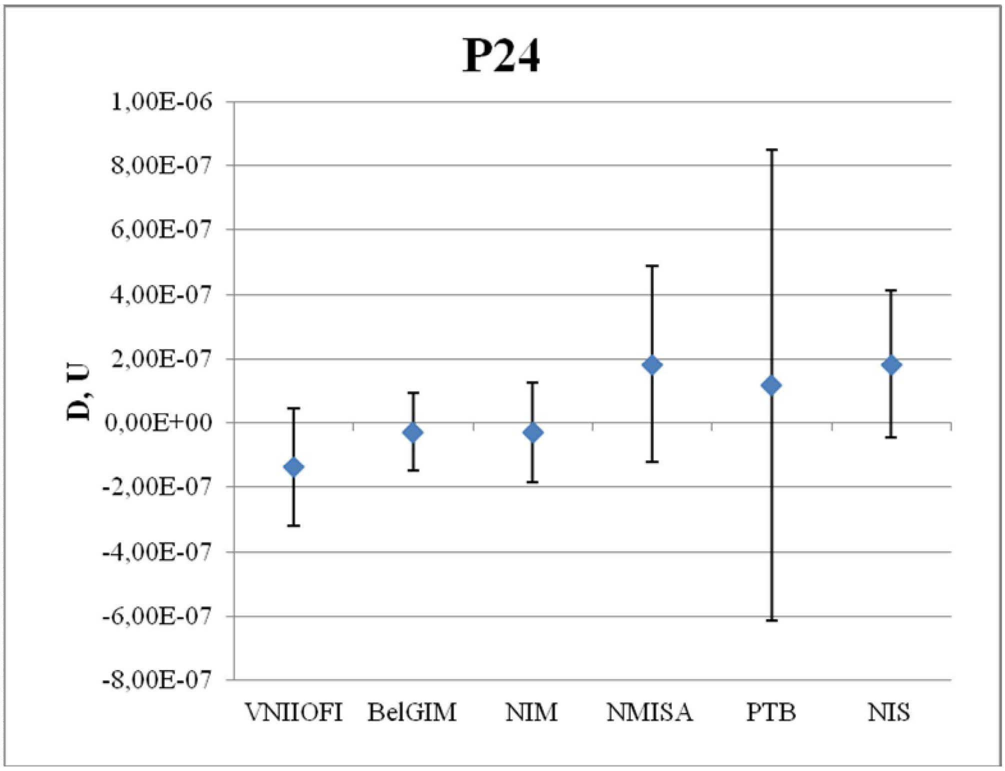

Fig. 6-11 – Relative deviation of the wavelength P24 from the CRV and combined standard uncertainties of participants.

Table 6-34 – The relative unilateral degree of equivalence and its uncertainty of each participant for P26.

P26	VNIIOFI	BelGIM	NIM	NMISA	PTB	NIS
Δ_i	0	-2,8142E-07	-2,68628E-07	-1,91877E-07	-4,47714E-07	-1,91877E-07
Δ_{CRV}	-2,07310E-07	-2,07310E-07	-2,07310E-07	-2,07310E-07	-2,07310E-07	-2,07310E-07
D_i	2,07310E-07	-7,41098E-08	-6,13179E-08	1,54330E-08	-2,40403E-07	1,54330E-08
$u(\Delta_i)$	1,89749E-07	9,03938E-08	1,51670E-07	3,02867E-07	7,29127E-07	2,58488E-07
$u_{adj}(\Delta_i)$	1,89749E-07	1,43414E-07	1,51670E-07	3,02867E-07	7,29127E-07	2,58488E-07
$u(\Delta_{\mathrm{CRV}})$	8,40624E-08	8,40624E-08	8,40624E-08	8,40624E-08	8,40624E-08	8,40624E-08
U_i	3,43641E-07	1,98543E-07	2,57072E-07	5,83940E-07	1,44934E-06	4,91258E-07

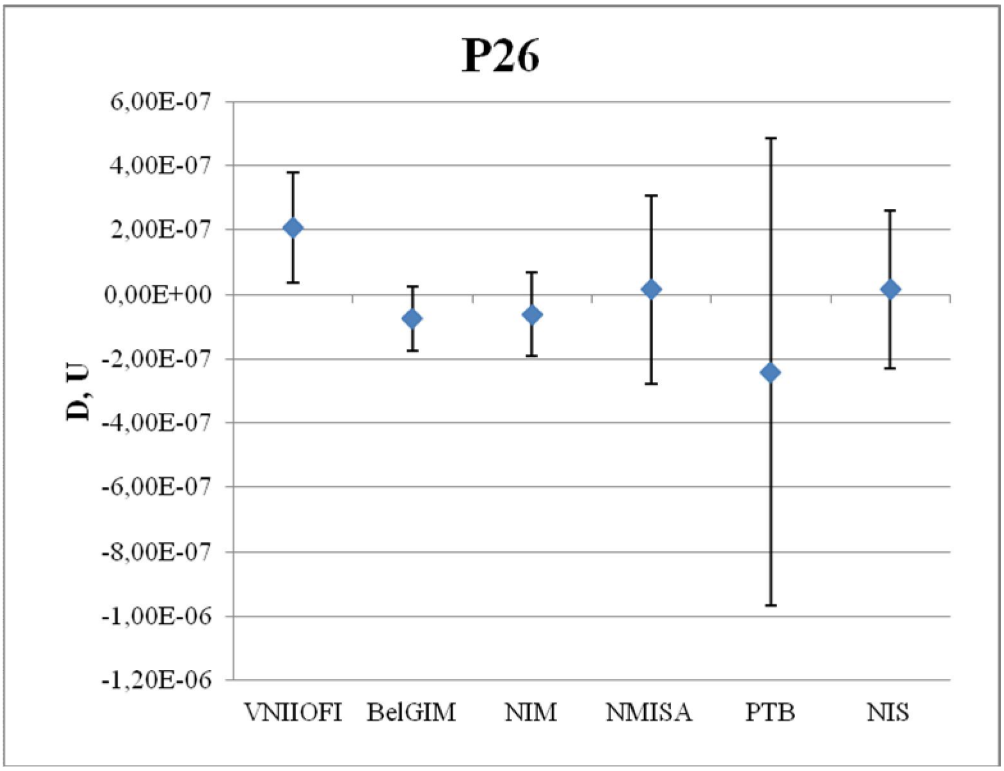

Fig. 6-12 – Relative deviation of the wavelength P26 from the CRV and combined standard uncertainties of participants.

Wavelength values and expanded uncertainties in absolute units for each wavelength are presented in tables 6-35 – 6-45:

Table 6-35 – Wavelength values and expanded uncertainties for R26

Wave-length peak	Organiza-tion	Wave-length	Expanded uncertainty in relative values	Expanded uncertainty in absolute values, nm	DoE	DoE in absolute values, nm
R26	VNIIOFI	1527,6336	3,52792E-07	5,38936E-04	9,04566E-09	1,38185E-05
	BelGIM	1527,6335	1,66901E-07	2,54964E-04	-4,04649E-09	-6,18155E-06
	NIM	1527,6335	2,40354E-07	3,67174E-04	-1,05926E-08	-1,61815E-05
	NMISA	1527,6335	5,87988E-07	8,98230E-04	-2,36847E-08	-3,61815E-05
	PTB	1527,6336	1,46561E-06	2,23892E-03	4,17760E-08	6,38185E-05
	NIS	1527,6336	4,91268E-07	7,50477E-04	4,17760E-08	6,38185E-05

Table 6-36 – Wavelength values and expanded uncertainties for R24

Wave-length peak	Organiza-tion	Wave-length	Expanded uncertainty in relative values	Expanded uncertainty in absolute values, nm	DoE	DoE in absolute values, nm
R24	VNIIOFI	1528,4859	2,80476E-07	4,28704E-04	-1,22984E-08	-1,87979E-05
	BelGIM	1528,4859	1,73014E-07	2,64449E-04	-3,19256E-08	-4,87979E-05
	NIM	1528,4859	2,65744E-07	4,06186E-04	-2,53832E-08	-3,87979E-05
	NMISA	1528,4862	5,98546E-07	9,14870E-04	1,83974E-07	2,81202E-04
	PTB	1528,4855	1,47093E-06	2,24830E-03	-2,73995E-07	-4,18798E-04
	NIS	1528,4860	2,95053E-07	4,50984E-04	5,31258E-08	8,12021E-05

Table 6-37 – Wavelength values and expanded uncertainties for R16

Wave-length peak	Organiza-tion	Wave-length	Expanded uncertainty in relative values	Expanded uncertainty in absolute values, nm	DoE	DoE in absolute values, nm
R16	VNIIOFI	1532,2830	2,86807E-07	4,39470E-04	-8,27574E-08	-1,26808E-04
	BelGIM	1532,2832	1,63428E-07	2,50417E-04	2,81881E-08	4,31922E-05
	NIM	1532,2832	2,64012E-07	4,04541E-04	1,51357E-08	2,31922E-05
	NMISA	1532,2830	5,96587E-07	9,14141E-04	-8,27574E-08	-1,26808E-04
	PTB	1532,2831	1,46971E-06	2,25202E-03	-1,74954E-08	-2,68078E-05
	NIS	1532,2832	2,93355E-07	4,49503E-04	4,77667E-08	7,31922E-05

Table 6-38 – Wavelength values and expanded uncertainties for R08

Wave-length peak	Organiza-tion	Wave-length	Expanded uncertainty in relative values	Expanded uncertainty in absolute values, nm	DoE	DoE in absolute values, nm
R08	VNIIOFI	1536,7037	2,73652E-07	4,20522E-04	-3,07552E-08	-4,72616E-05
	BelGIM	1536,7037	1,67084E-07	2,56759E-04	-2,42477E-08	-3,72616E-05

Wave-length peak	Organiza-tion	Wave-length	Expanded uncertainty in relative values	Expanded uncertainty in absolute values, nm	DoE	DoE in absolute values, nm
	NIM	1536,7036	2,57910E-07	3,96331E-04	-5,67849E-08	-8,72616E-05
	NMISA	1536,7038	5,92526E-07	9,10537E-04	6,68564E-08	1,02738E-04
	PTB	1536,7033	1,46758E-06	2,25524E-03	-2,58515E-07	-3,97262E-04
	NIS	1536,7039	2,87712E-07	4,42129E-04	1,31931E-07	2,02738E-04

Table 6-39 – Wavelength values and expanded uncertainties for R00

Wave-length peak	Organiza-tion	Wave-length	Expanded uncertainty in relative values	Expanded uncertainty in absolute values, nm	DoE	DoE in absolute values, nm
R00	VNIIOFI	1541,7528	2,98297E-07	4,59901E-04	5,85949E-08	9,03389E-05
	BelGIM	1541,7526	1,87398E-07	2,88922E-04	-3,86970E-08	-5,96611E-05
	NIM	1541,7526	2,69082E-07	4,14858E-04	-7,11276E-08	-1,09661E-04
	NMISA	1541,7528	5,95915E-07	9,18753E-04	9,10255E-08	1,40339E-04
	PTB	1541,7523	1,46840E-06	2,26391E-03	-2,33281E-07	-3,59661E-04
	NIS	1541,7528	3,67201E-07	5,66134E-04	9,10255E-08	1,40339E-04

Table 6-40 – Wavelength values and expanded uncertainties for P05

Wave-length peak	Organiza-tion	Wave-length	Expanded uncertainty in relative values	Expanded uncertainty in absolute values, nm	DoE	DoE in absolute values, nm
P05	VNIIOFI	1545,9558	2,79174E-07	4,31590E-04	4,23735E-08	6,55076E-05
	BelGIM	1545,9557	1,65280E-07	2,55516E-04	-5,46539E-08	-8,44924E-05
	NIM	1545,9557	2,58518E-07	3,99657E-04	-3,52484E-08	-5,44924E-05
	NMISA	1545,9558	5,89920E-07	9,11990E-04	4,23735E-08	6,55076E-05
	PTB	1545,9556	1,47758E-06	2,28427E-03	-8,69963E-08	-1,34492E-04
	NIS	1545,9559	3,59060E-07	5,55091E-04	1,07058E-07	1,65508E-04

Table 6-41 – Wavelength values and expanded uncertainties for P10

Wave-length peak	Organiza-tion	Wave-length	Expanded uncertainty in relative values	Expanded uncertainty in absolute values, nm	DoE	DoE in absolute values, nm
P10	VNIIOFI	1549,7303	2,80384E-07	4,34520E-04	-1,02174E-07	-1,58342E-04
	BelGIM	1549,7304	1,55547E-07	2,41056E-04	-2,47410E-08	-3,83419E-05
	NIM	1549,7305	2,54358E-07	3,94186E-04	3,97863E-08	6,16581E-05
	NMISA	1549,7306	5,86944E-07	9,09606E-04	1,23672E-07	1,91658E-04
	PTB	1549,7305	1,47209E-06	2,28134E-03	5,91445E-08	9,16581E-05
	NIS	1549,7305	2,84054E-07	4,40208E-04	5,91445E-08	9,16581E-05

Table 6-42 – Wavelength values and expanded uncertainties for P16

Wave-length peak	Organiza-tion	Wave-length	Expanded uncertainty in relative values	Expanded uncertainty in absolute values, nm	DoE	DoE in absolute values, nm
P16	VNIIOFI	1554,5904	2,82317E-07	4,38888E-04	-1,02375E-07	-1,59151E-04
	BelGIM	1554,5906	1,70813E-07	2,65545E-04	-5,88633E-09	-9,15084E-06
	NIM	1554,5905	2,60596E-07	4,05121E-04	-1,87515E-08	-2,91508E-05
	NMISA	1554,5908	5,88192E-07	9,14397E-04	1,54928E-07	2,40849E-04
	PTB	1554,5906	1,46390E-06	2,27577E-03	2,62765E-08	4,08492E-05
	NIS	1554,5907	2,89481E-07	4,50025E-04	9,06021E-08	1,40849E-04

Table 6-43 – Wavelength values and expanded uncertainties for P24

Wave-length peak	Organiza-tion	Wave-length	Expanded uncertainty in relative values	Expanded uncertainty in absolute values, nm	DoE	DoE in absolute values, nm
P24	VNIIOFI	1561,6355	3,65195E-07	5,70302E-04	-1,36719E-07	-2,13506E-04
	BelGIM	1561,6357	2,40401E-07	3,75419E-04	-2,78593E-08	-4,35060E-05
	NIM	1561,6357	3,10716E-07	4,85225E-04	-2,78593E-08	-4,35060E-05
	NMISA	1561,6360	6,10000E-07	9,52598E-04	1,83458E-07	2,86494E-04
	PTB	1561,6359	1,46402E-06	2,28626E-03	1,19422E-07	1,86494E-04
	NIS	1561,6360	4,59024E-07	7,16829E-04	1,83458E-07	2,86494E-04

Table 6-44 – Wavelength values and expanded uncertainties for P26

Wave-length peak	Organiza-tion	Wave-length	Expanded uncertainty in relative values	Expanded uncertainty in absolute values, nm	DoE	DoE in absolute values, nm
P26	VNIIOFI	1563,4988	3,43641E-07	5,37283E-04	2,07310E-07	3,24129E-04
	BelGIM	1563,4984	1,98543E-07	3,10422E-04	-7,41098E-08	-1,15870E-04
	NIM	1563,4984	2,57072E-07	4,01932E-04	-6,13179E-08	-9,58705E-05
	NMISA	1563,4985	5,83940E-07	9,12989E-04	1,54330E-08	2,41295E-05
	PTB	1563,4981	1,44934E-06	2,26603E-03	-2,40403E-07	-3,75870E-04
	NIS	1563,4985	4,91258E-07	7,68081E-04	1,54330E-08	2,41295E-05

Conclusion

We report the results of the supplementary comparison on COOMET PR-S8 Project among BelGIM, NIM, NIS, NMISA, PTB and VNIIOFI (pilot) on wavelengths for fiber optics within wavelength range from 1525 to 1565 nm.

At the final stage of predraft A discussion, INMETRO which was the initial participant and made the measurements according to the technical protocol, decided to discontinue participation. NIS was included as additional participant by all participants' agreement.

The artifact based on a Hydrogen Cyanide ($H^{13}C^{14}N$) gas cell had been selected to provide the absorption peaks within the wavelength range from 1525 to 1565 nm which is most important for telecommunication. The instability (drift) of artifact (about 0,2 pm) is small enough; it was considered when calculating as additional uncertainty for every participant.

The wavelengths of ten absorption peaks have been measured by all participants and compared. We obtained consistent results for all wavelength absorption peaks for all participants.

The maximum relative deviation from CRV for all participants and at all wavelengths doesn't exceed 2,74E-07 or in absolute units – 0,42 pm. There are no points with great deviations according to paragraph 4.2 of [1]. It is concluded, therefore, that results of intercomparison are uniform and satisfactory for whole wavelength range.

With regard to CMC claim on the items 7.2.0, 7.2.1, 7.2.2 of CCPR service categories that are wavelength / sources, wavelength / spectrum analyzers, wavelength / wavelengths meters, this comparison report can be used to support it as evidence.

References

1 Guideline for CCPR Key Comparison Report Preparation, CCPR Working Group on Key Comparisons CCPR-G2, Rev.3, July 1, 2013.

2 ISO/IEC Guide 98-3:2008 "Measurement uncertainty – Part 3: Guide on measurement uncertainty expression (GUM: 1995)".

3 W. C. Swann and S. L. Gilbert "Line centers, pressure shift, and pressure broadening of 1530–1560 nm hydrogen cyanide wavelength calibration lines," J. Opt. Soc. Am. B **22**,1749-1756 (2005).

4 S. Falke, H. Schnatz, J.S.R. Vellore Winfred, T. Middelmann, S. Vogt, S. Weyers, B. Lipphardt, G. Grosche, F. Riehle, U. Sterr und C. Lisdat, „The ^{87}Sr optical frequency standard at PTB", Metrologia, **48**, 399-407 (2011).

5 L. Robertsson, M. Zucco, L-S. Ma, O. Terra, F. Saraiva, S. Gentil, C. Chekirda, Yu Zakharenko, V. Fedorin and L. Mostert "Results from the CI-2004 campaign at the BIPM of the BIPM.L-K11 ongoing key comparison" Metrologia 42 (2005).

6 O. Terra and H. Hussein, "An ultra-stable optical frequency standard for telecommunication purposes based upon the 5S1/2 → 5D5/2 two-photon transition in Rubidium", Applied Physics B, 122: 27. doi:10.1007/s00340-015-6309-4 (2016).

7 O. Terra and H. Hussein, "Calibration of grating-based optical spectrum analyzers", Journal of Optics, vol. 44, Issue 4 pp. 366-372 (2015).